ANL-5950
Reactors - Power
(TID-4500, 15th Ed.)
AEC Research and
Development Report

ARGONNE NATIONAL LABORATORY
P. O. Box 299
Lemont, Illinois

CASTING AND FABRICATION OF CORE MATERIAL FOR ARGONNE LOW POWER REACTOR FUEL ELEMENTS

by

R. L. Salley and W. R. Burt, Jr.

Metallurgy Division
Program 7.6.8

A portion of the material contained in this report has been reported in the following Metallurgy Division Report: ANL-5975, pp. 12-13, March, 1959.

December, 1959

Operated by The University of Chicago
under
Contract W-31-109-eng-38

DISCLAIMER

TABLE OF CONTENTS

LIST OF TABLES

LIST OF FIGURES

LIST OF FIGURES

CASTING AND FABRICATION OF CORE MATERIAL FOR ARGONNE LOW POWER REACTOR FUEL ELEMENTS

by

R. L. Salley and W. R. Burt, Jr.

ABSTRACT

The Argonne Low Power Reactor (ALPR) is fueled currently with thin, plate-type elements containing a wrought, aluminum-base core alloy, with a nominal composition of 17.5 w/o fully enriched uranium, 2.0 w/o nickel, and 0.5 w/o iron, clad with an aluminum-nickel alloy. Fuel elements were fabricated by a picture-frame technique, employing elemental silicon bonding. Following this operation the compacts were hot and cold rolled to final size.

This report describes the manufacture of 1150 fuel core blanks, of which 816 were used in the fabrication of fuel elements. Development, casting, hot and cold rolling, cleaning, and punching of core blanks are discussed, as are nondestructive testing and evaluation of the manufacturing processes.

INTRODUCTION

The specified fuel for the Argonne Low Power Reactor (ALPR) was an aluminum alloy plate-type element. Each plate was to contain 39 ± 1 gm U^{235} in an aluminum-nickel matrix and clad with an aluminum-1 w/o Ni alloy (X-8001). The specification of highly enriched uranium together with the final core size required a core alloy composition of 17.5 w/o U, 2.0 w/o Ni, balance 2S aluminum, to obtain 39 gm U^{235} per plate. The finished fuel plates were 0.120 in. thick, 4.6 in. wide, and 27.8 in. long, and contained a 0.050 in. thick, $3\frac{1}{2}$ to $3\frac{9}{16}$ in. wide and $25.8 \pm \frac{1}{2}$ in. long uranium-bearing core. Fuel plates were fabricated by the picture-frame technique, starting with a 0.200 in. thick, 3.316 in. wide, and 6.875 in. long core blank.[1] This report deals with the manufacture of these core blanks.

Fabrication of the enriched uranium core blanks basically consisted of melting and casting, rolling, punching, and inspection. As time was limited, some of the development work was performed concurrently with production of enriched core material.

In addition to the actual manufacturing processes, this report describes the problems encountered - casting soundness and homogeneity, edge cracking during rolling, and determination of U^{235} content per core - and their solutions.

CORE ALLOY PROCESSING

Development

The major problems in producing the aluminum core alloy were twofold: first, the selection of a mold to produce a sound and homogeneous casting suitable for fabrication; and second, the establishment of melt cycles for producing castings in two furnaces varying in capacity. While previous work on Al-U alloys did offer solutions to the problems of porosity and segregation,[2] the peculiar characteristics of individual furnaces require development of the proper melt cycle for each furnace.

The initial attempts to produce sound, homogeneous castings were made by casting into a slab-type graphite mold, $1\frac{1}{2}$ x $7\frac{1}{2}$ in. in cross section and 8 in. deep. The resultant castings consistently exhibited major segregation and cracked severely in hot rolling. Although this segregation was reduced through varying the melting and casting conditions, sufficient improvement in homogeneity to provide acceptable material for fabrication was not realized, and the slab casting was abandoned in favor of a mold having a cross section of 2 x 4 in. and a depth of $18\frac{1}{2}$ to $19\frac{1}{2}$ in. This mold presented more favorable conditions for obtaining sound homogeneous castings in that directional solidification (vertical) could be obtained more readily.

The established rate of production required the foundry to produce two 2 x 4 x $18\frac{1}{2}$ in. castings per day. Three quartz tube, vacuum induction furnaces were available. Two of these, identical and larger than the third, had a quartz tube of 22-in. OD. The third had a 13-in. OD quartz tube and is described in detail later in the report.

The first melt cycle to be established was for the 13-in. quartz tube furnace. Establishing a melt cycle for the larger furnaces proved more difficult due to: (1) the longer time required to attain the prescribed heat temperature (an average of 55 min to begin melting the aluminum, as compared to 12 min in the small furnace), and (2) the greater radiation of heat from the crucible to the mold in the larger furnace. The mold temperature gradient developed during a heat in the 13-in. furnace could not be reproduced in the large furnace despite efforts to isolate the mold from the crucible. A total of eighteen castings were produced in the larger furnace and all were rejected because of porosity or segregation. Larger crucibles were used in order to decrease the heating time, but this had little effect

and, in one instance, resulted in longer heating time. While casting soundness and homogeneity were improved, the results were inferior compared to the quality obtained by use of the 13-in. furnace. Consequently, the use of the large furnaces was abandoned and production rates were met by incorporating a two-shift work day, producing one casting per shift in the 13-in. furnace.

Charge Material

The composition of an ALPR core plate was flexible in that its composition was dependent on its volume. Specifications required that each plate contain 39 $\pm$ 1 gm U^{235}, 2.0 $\pm$ 0.2 w/o Ni, 0.5 $\pm$ 0.1 w/o Fe, and the balance aluminum.

The materials specified for producing the ALPR core alloy were 1100 aluminum, nickel, and enriched uranium having a minimum U^{235} isotopic concentration of 91%.

The necessary uranium content to furnish 39 gm U^{235} per plate was calculated on the basis of core volume and densities of the alloy constituents. The resultant charge composition was 17.5 w/o uranium enriched in U^{235} to 93.2%, 2.0 w/o nickel, and 80.5 w/o 1100 aluminum. The iron content of the 1100 aluminum was sufficient to comply with the 0.5 w/o specification for the core alloy.

The total charge weight was fixed to fill the mold and hot top, whose dimensions were 2 x 4 x 19$\frac{1}{2}$ in. and 4 in. dia x 1 in., respectively. The average charge weight was approximately 8,250 gm and a typical charge is illustrated in Figure 1.

The aluminum was received in the form of pigs which had to be sectioned into pieces that could be readily charged into the crucible. The pigs were cut into 1, 1$\frac{1}{2}$, and 2-in. thick slices having a cross section approximately 4$\frac{1}{2}$ x 5 in. These slices were then cut in half and wire brushed to remove all burrs and loose filings to facilitate weighing to the nearest milligram. Brushing was done with an 8-in. diameter wheel mounted on a $\frac{1}{2}$-hp motor.

The aluminum originally supplied was commercially pure aluminum. Unaware of this error, this aluminum was used in producing the first eight castings. In addition to porosity, these castings had a low iron content, averaging about 0.1 w/o. A spectrochemical analysis of the aluminum showed an iron content of 0.07 w/o, indicating the material to be commercially pure aluminum rather than 1100.

To continue casting production while awaiting delivery of a shipment of 1100 aluminum, an aluminum-nickel alloy, X-8001, was used as melting stock. Chemical analyses of this material showed a nickel content

FIGURE 1. Typical ALPR Virgin Charge: 1100 aluminum, nickel shot, enriched uranium

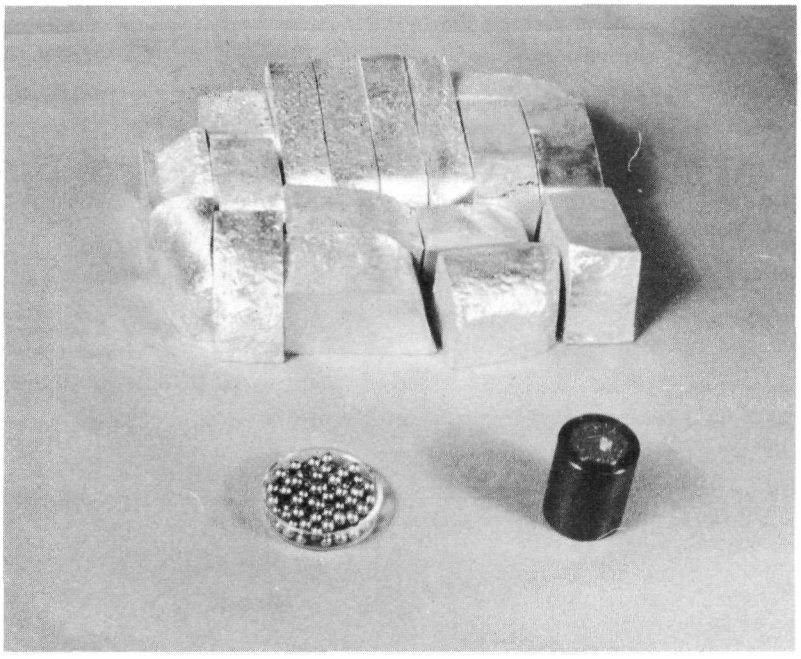

106-4318

ranging from 1.02 to 1.10 w/o and an iron content ranging from 0.49 to 0.52 w/o. Specifications for X-8001 call for 0.9-1.1 w/o Ni; therefore, a nominal 1.0 w/o was assumed in calculating the amount of nickel shot to be added to the charge. The X-8001 alloy was scrap and defective material from the production of picture-frame and cladding stock to be used for fuel-plate fabrication.

The nickel added was "Baker Analyzed Reagent" shot containing 0.043% impurities, the major impurity being 0.04% iron which, in this case, was beneficial.

The enriched uranium initially was added as chunks of as-received biscuit, later as pickled biscuit material, and finally as premelted stock. The first eight enriched castings were rejected because of severe porosity in addition to a low iron content. These castings were produced under the same melting and casting conditions as were the final development castings, which were free of porosity. Although the aluminum and nickel melt stocks were the same for both development and enriched castings, the former were charged with premelted natural uranium (0.7% U^{235}) while as-received biscuit uranium was charged to the enriched melts. The supposition was then made that the porosity occurring in the first three enriched-uranium castings might be due to the heavily oxidized, enriched biscuit uranium,

inasmuch as the use of premelted normal uranium resulted in sound castings. To remedy this, the as-received biscuit uranium was pickled in a 50% nitric bath at 80°C to remove the heavy oxide layer and other entrapped impurities. Use of this pickled uranium biscuit in producing three more castings proved fruitless, as all exhibited porosity. Remelting two of the six porous castings previously made did not eliminate the porosity, although it was lessened to some degree.

Spectrochemical analysis of as-received enriched biscuit uranium revealed that a considerable amount of calcium (more than 1000 ppm) was present. This contaminant resulted from the bomb reduction of uranium salt to biscuit metal. Since this element is volatile at elevated temperatures, it can be removed by melting the uranium in a high vacuum. Removal of calcium is indicated in Table I, where minor element contents of as-received biscuit and premelted uranium are tabulated. Magnesium content was reduced by a factor of 30, as well. Also during melting, any entrapped gases can escape and oxides and other contaminants can form a skull which will float on the surface of the molten uranium. Separation of the purified uranium from the skull can best be accomplished by bottom pour casting, as the skull will remain in the crucible.

TABLE I. Impurity Content of As-received and Premelted Enriched Uranium

Impurity	Impurity Content, ppm*		Impurity	Impurity Content, ppm*	
	As-received Biscuit	Premelted Casting		As-received Biscuit	Premelted Casting
Ag	L1	L1	Mg	100	3
Al	10	5	Mn	2	1
As	L10	L10	Mo	L20	30
B	L0.1	L0.1	Na	L10	L10
Be	L0.5	L0.5	Ni	30	10
Bi	L1	L1	P	L50	L50
Ca	G1000	L20	Pb	L1	L1
Co	L5	L5	Sb	L1	L1
Cr	2	2	Si	15	80
Cu	70	4	Sn	L5	L5
Fe	40	40	Ti	L50	L50
K	L50	L50	Zn	L50	L50
Li	L1	L1			

*L indicates less than

The use of enriched uranium which had been premelted in vacuo resulted in a sound ALPR casting. Consequently all subsequent virgin charges consisted of premelted stock.

The premelting was done in a $5\frac{5}{8}$-in. diameter Vycor tube, high vacuum, induction furnace utilizing a 15-kw, high-frequency, motor-generator set. Power from this set was induced into the furnace by means of a coil surrounding the Vycor tube. This coil was 7 in. high x $6\frac{3}{4}$ in. OD and consisted of 13 turns of $\frac{3}{8}$-in. OD copper tubing. Power was transmitted from the generator to the furnace by means of a 4 x $\frac{1}{4}$-in. cross-sectional, water-cooled, copper bus bar.

The as-received biscuit uranium was charged into a $3\frac{1}{8}$-in. diameter, $7\frac{1}{2}$-in. deep, high-purity MgO bottom pour crucible. Larger melts later necessitated use of a 4-in. high, magnesia crucible extension. A $\frac{5}{8}$-in. diameter, high-purity MgO stopper rod with a tapered point was fitted into a $\frac{3}{8}$-in. diameter pouring hole. A $3\frac{1}{8}$-in. diameter, $\frac{3}{8}$-in. thick, high-purity MgO cover with a $\frac{3}{4}$-in. diameter sight hole was placed over the crucible after loading. A 0.030-in. thick tantalum susceptor encased the crucible and cover and was, in turn, surrounded by a $\frac{3}{8}$-in. thick, 10-in. high zirconia insulator. A magnesia spacer was used between the crucible and mold.

The metal was cast into a split cylindrical graphite mold, tapered compression rings being used to hold the mold together. The mold dimensions were $2\frac{3}{4}$ in. OD, $1\frac{3}{4}$ in. ID, and a 9-in. internal depth. The mold cavity was covered with a $MgZrO_3$ wash.

Though the furnace was capable of operating with a vacuum of 1×10^{-6} mm Hg, power was applied when a minimum vacuum of 4×10^{-4} mm Hg was obtained. A typical melt cycle consisted of heating the metal to 1400°C, holding at this temperature for $\frac{1}{2}$ hr, lowering the temperature to 1300°C, and pouring. At the time of pouring, the vacuum was 2×10^{-4} mm Hg or better in all melts. The weight of enriched uranium biscuit charged varied from 3617 to 8065 gm.

After the castings were removed from the mold, they were weighed and cleaned for notching and breaking. Cleaning to remove adhering wash or oxide film was best accomplished by making a light skin cut on the circumferential surface of the casting (billet). The billet was then weighed again and its longitudinal length measured to determine its weight per linear inch. The billet could now be notched and broken into segments of predetermined weights for charging to the core alloy melts.

Notching of the billet was accomplished by machining a circumferential groove in the billet measuring $\frac{1}{8}$ in. wide and $\frac{3}{8}$ in. deep. Machining was done on a 12-in Monarch lathe using a carboloy-tipped parting tool. The notched billet was then immersed in a thermos containing liquid nitrogen.

When the casting reached the liquid nitrogen temperature (-196°C, it was removed and broken at the notch in a protective hood on a 10-ton Greenerd arbor press using a "V"-nose tip at the end of the hydraulic ram, as shown in Figures 2A and 2B. Depending on the pattern of fracture, it was sometimes necessary to machine the piece further to the correct charge weight or to add additional small pieces of premelted uranium.

Crucibles

The melting and alloying of the aluminum-uranium-nickel alloy were done in graphite, bottom-pour crucibles, protected from attack by the melt by a duplex ceramic coating. The crucible, shown in Figure 3 and detailed in Figure 4, measured 8 in. in outside diameter, 10 in. in overall height, and $\frac{1}{2}$ in. in wall thickness. The interior height of $9\frac{1}{8}$ in. had a one-degree pitch to facilitate draining of the melt and removal of the skull. The interior bottom also was tapered to the pouring hole to assist in draining.

The $\frac{3}{4}$-in. diameter, ceramic-coated, graphite stopper rod fitted into the $\frac{3}{8}$-in. diameter pouring hole by means of a $\frac{3}{8}$-in. long, $\frac{5}{16}$-in. diameter tapered tip. The rod was designed to permit slight movement, either vertically or horizontally, without allowing leakage of molten metal from the crucible, being manipulated by a $\frac{1}{4}$-in. diameter tantalum pull rod fastened to the stopper rod by a tantalum clevis and pin. The pull rod passed through a compression-type vacuum seal in the furnace cover. All crucibles and stopper rods were made from ATZ grade graphite.

It was necessary to protect the graphite crucible and stopper rod from attack by the molten metal. Protection was provided in the form of a duplex ceramic coating. The base coating was a slurry of magnesium zirconate which was applied by brushing in two layers, with approximately $1\frac{1}{2}$ to 2 hours of drying time between applications. Two medium layers of $MgZrO_3$ are preferable to a single heavy layer, as the latter tends to crack on drying. The second, or top, coating consisted of a suspension of thoria in water, which was applied by spraying. Both crucibles and stopper rods were allowed to air dry before they were placed in the furnace.

The $MgZrO_3$ was supplied by the Titanium Alloy Manufacturing Division and the Code 112 ThO_2 by the Lindsay Chemical Company. The thoria had been fired at 800°C and averaged in particle size between 0.5 and 2.0 microns.

In no instance did the molten metal break through the wash and attack the graphite. After casting, the crucible was removed from the furnace and the melt residue or skull salvaged. The ceramic coating was scraped from the crucible and stopper rod and stored as contaminated material. The surfaces of the crucible and stopper rod were then cleaned and recoated prior to reuse.

FIGURE 2. Breaking of Chilled Uranium Casting into Predetermined Segments by a "V"-Nosed Hydraulic Ram

2A.

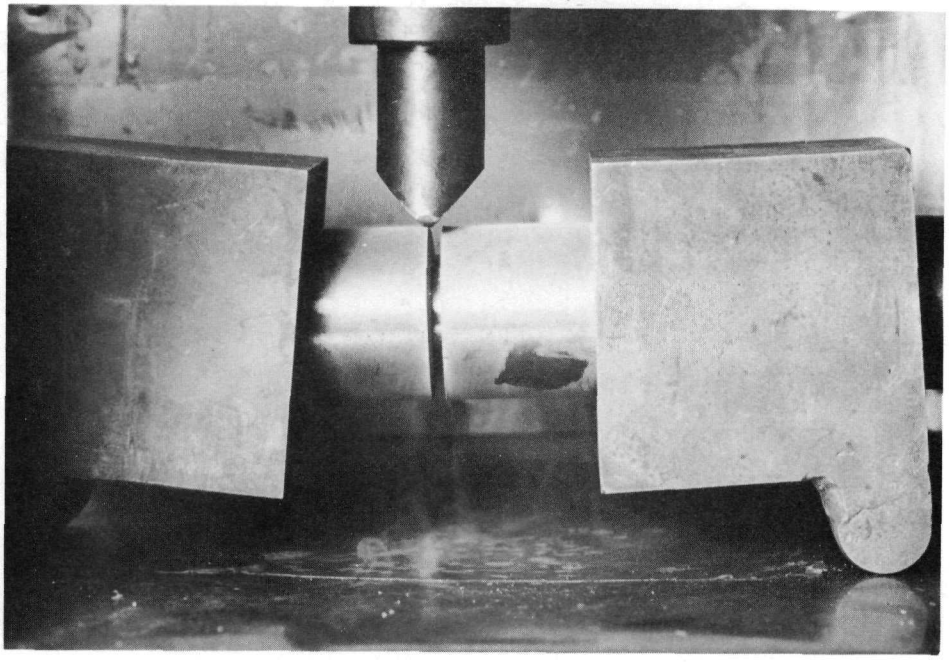

106-4177 Prior to Breaking

2B.

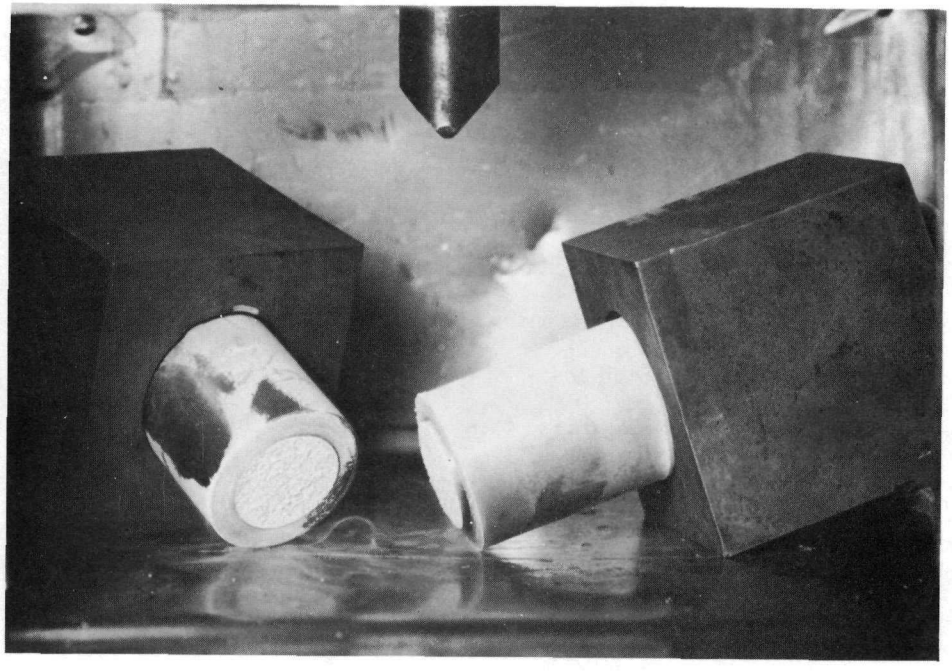

106-4180 After Breaking

FIGURE 3. Graphite Crucible and Stopper Rod with Duplex Ceramic Coating

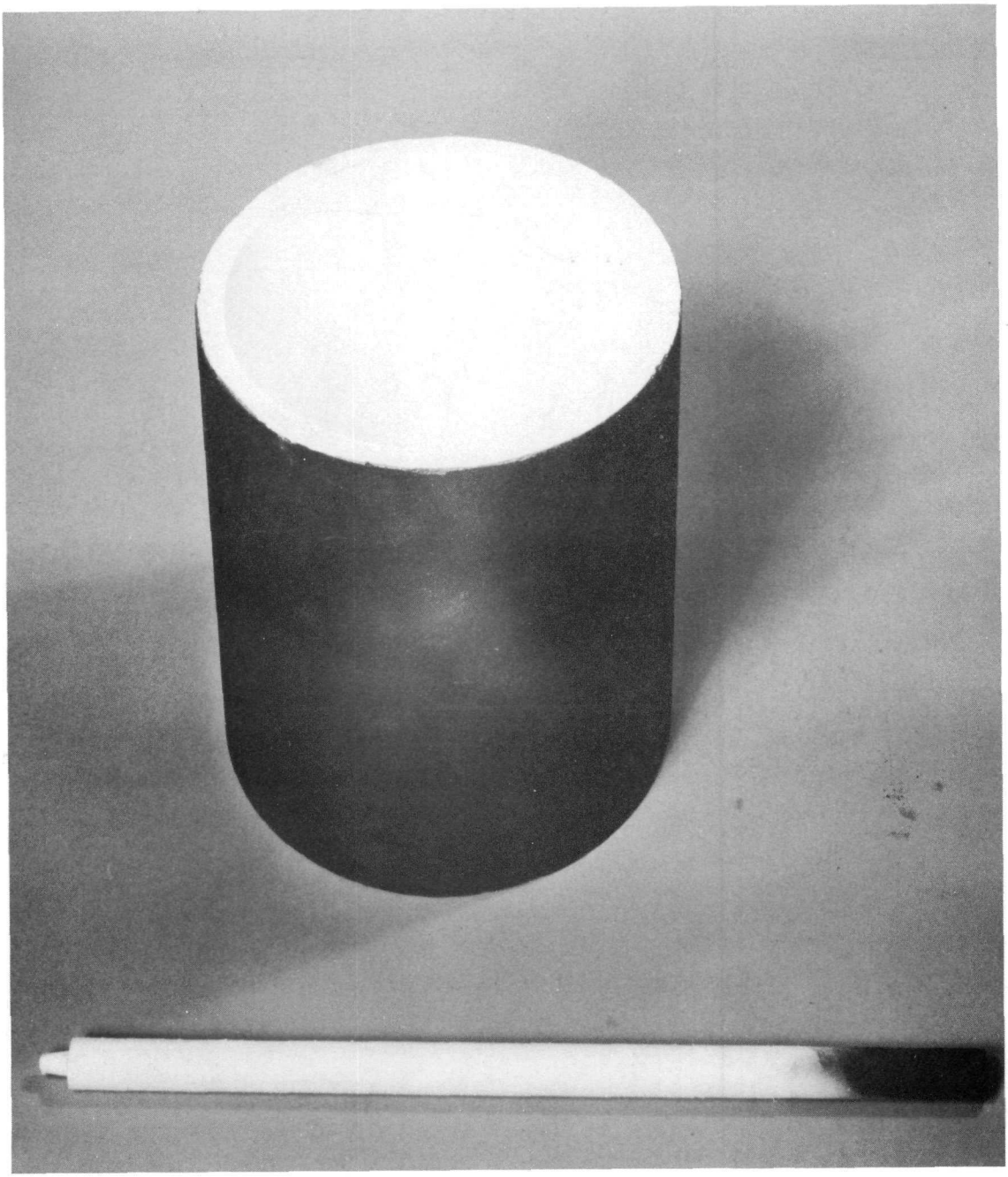

106-4182

(2) Graphite Crucible Cover

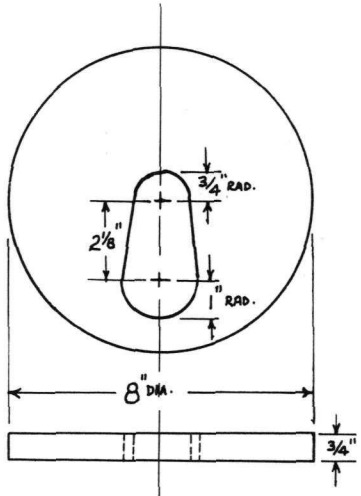

(4) Graphite Crucible

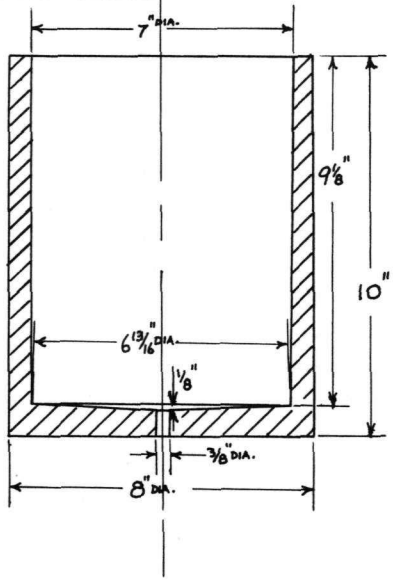

(1) Tantalum Stopper Rod Extension

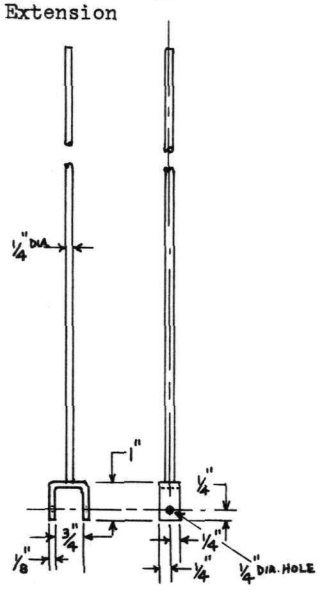

(3) Graphite Stopper Rod

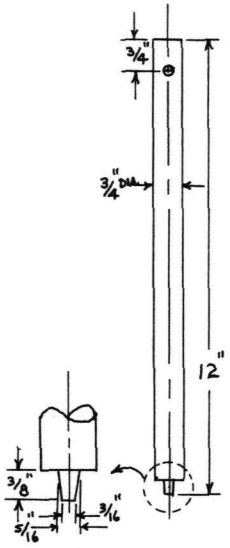

FIGURE 4. Design and Dimensions of Graphite Crucible, Cover, and Stopper Rod

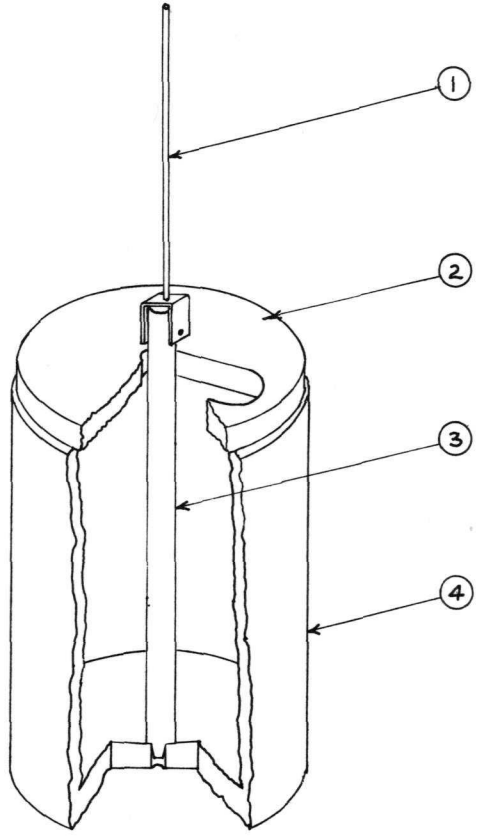

A total of eight crucibles and stopper rods were employed to make 68 enriched fuel alloy castings and approximately 25 development castings.

Molds

A split graphite mold (Figure 5) was used to produce the fuel alloy castings. When assembled, the mold formed a cylinder $5\frac{1}{4}$ in. in diameter and 22 in. high. The two halves were machined to form a cavity having cross-sectional dimensions of 2 x 4 in. with a $\frac{1}{4}$-in. radius at the corners. The two mold sections were held together by two tapered graphite rings serving as compression rings. A graphite plate, 2 x 4 x $\frac{1}{4}$ in., was inserted at the bottom of the mold and acted as a plug. This plate rested on a $\frac{3}{4}$-in. thick copper chill block which aided in initiating directional solidification of the cast metal.

Three 0.190-in. diameter holes were drilled in the mold to within $\frac{1}{8}$ in. of the inner mold wall at equal intervals along the mold length (see Figure 5 for spacing dimensions). Twin-bore ceramic tubing-insulated chromel-alumel thermocouples with bare beads were inserted in these holes to obtain top, middle, and bottom mold temperatures during a heat cycle. The thermocouples passed through compression-type vacuum seals in the furnace bottom.

The temperatures of mold and metal during a typical heat cycle are graphically illustrated in Figure 6. When the melt was ready for pouring, it was most important to have the mold temperature gradient indicated on the graph. This gradient was allowed to vary uniformly within +10 and -25°C of the indicated temperatures. With temperatures varying beyond these limits, porosity or severe segregation was likely to occur, porosity with the lower temperatures and segregation at the high temperatures. Figure 7 shows the X-ray radiographs and mold temperatures of two developmental castings made with mold temperatures varying beyond the desired limits.

One mold was used to produce all 68 fuel alloy castings. The alloy was cast into a bare mold, no ceramic wash being used. After removal of the casting from the mold, it was necessary only to lightly sandpaper the mold wall in preparation for the next heat. The graphite bottom plug had to be replaced five times in producing the castings. Erosion of the plate by the molten metal weakened it such that, after approximately 12 heats, the plate would crack when removing it from the casting.

Vacuum Induction Furnace

Melting, alloying, and casting of the ALPR fuel alloy were accomplished in a vacuum induction furnace, the furnace proper being a quartz tube with an exterior induction coil. The furnace was located on a balcony such that the tube, coil and furnace top were above the balcony floor for observation and control of heats. The furnace bottom and the

FIGURE 5. Design and Dimensions of ALPR Mold Assembly

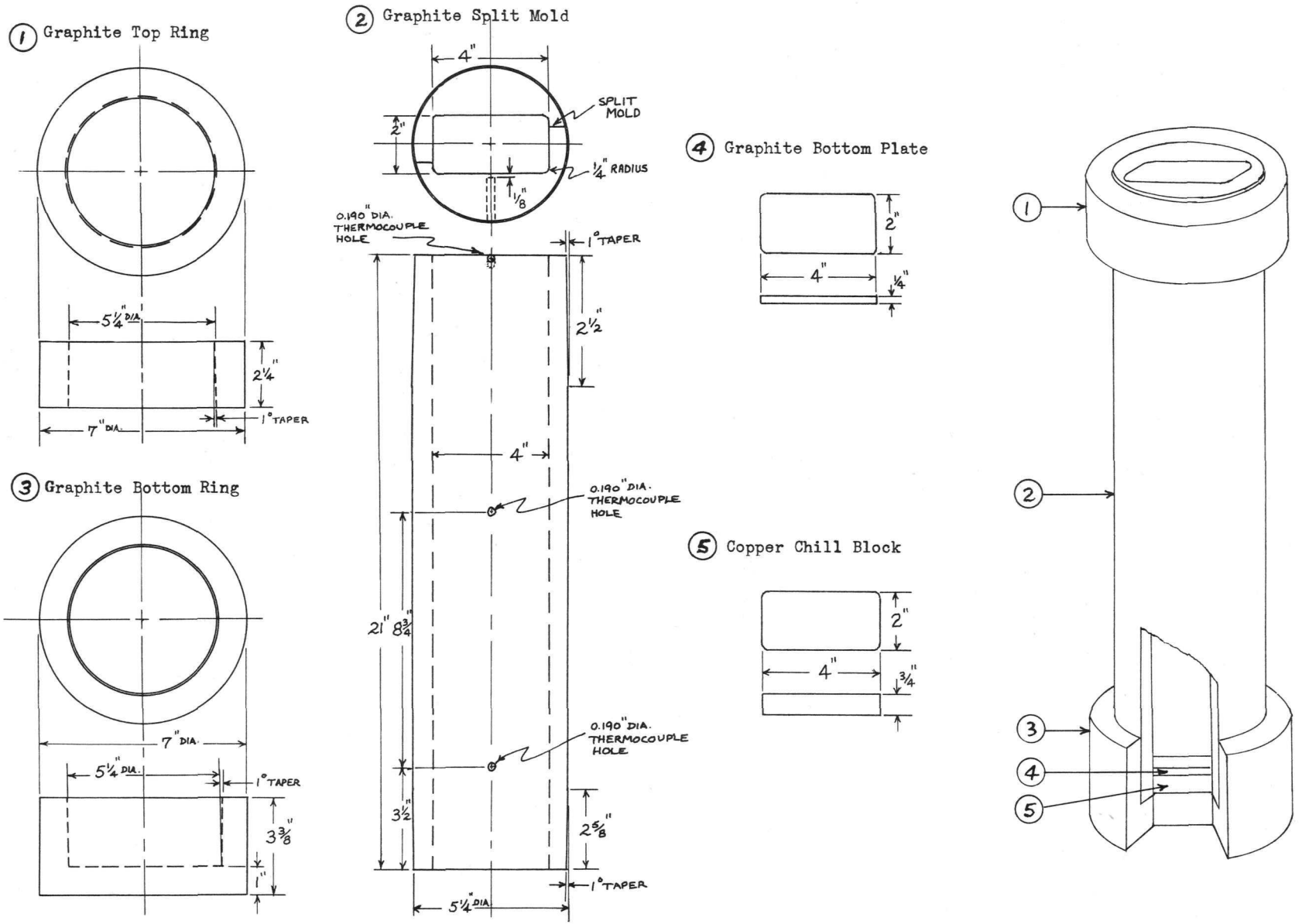

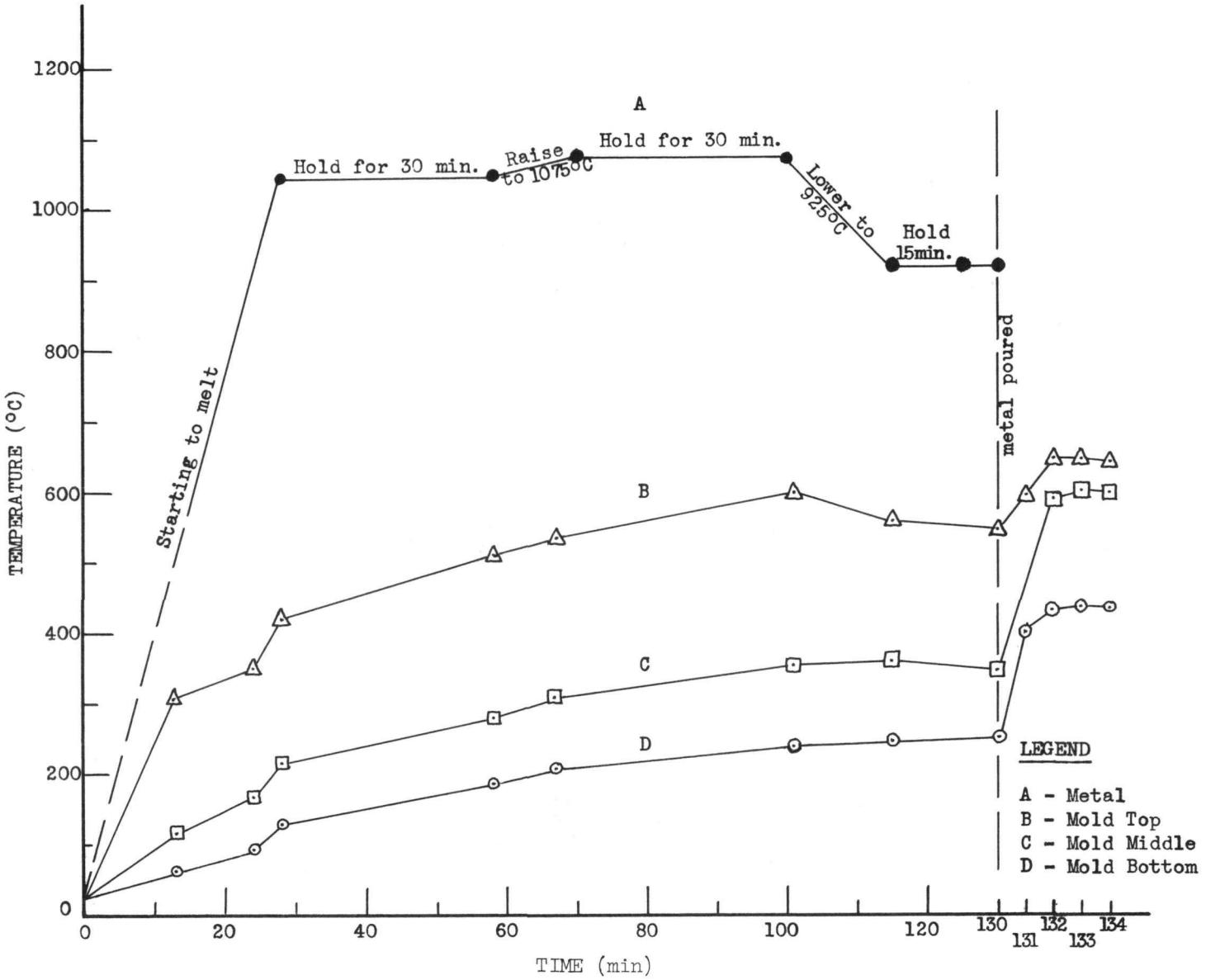

FIGURE 6. Metal and Mold Temperatures as a Function of Melt Time for Melt A19

FIGURE 7. X-ray Radiographs of Two Developmental Castings Whose Mold Temperatures Just Prior to Pouring Were beyond Specified Limits

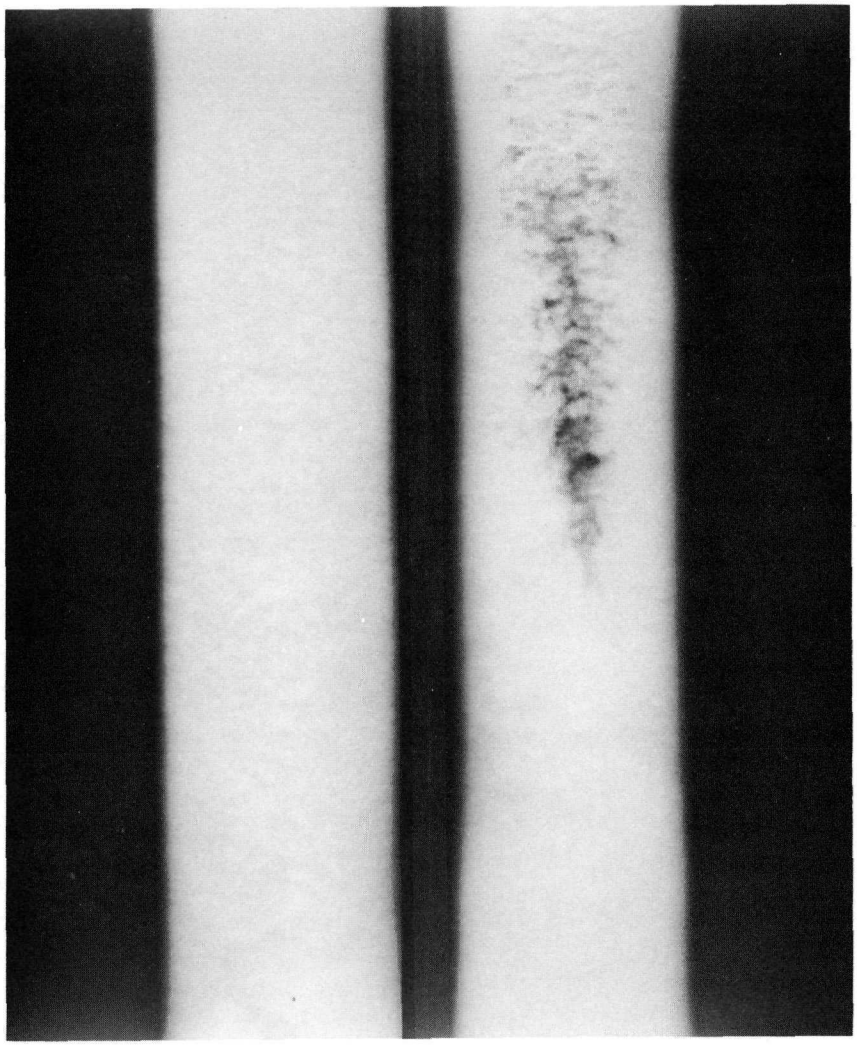

106-4319

	Mold Temperatures °C			
	Top	Center	Bottom	Defect
Left X-ray	620	494	412	Segregation
Right X-ray	496	356	272	Porosity
Desired	550^{+10}_{-25}	355^{+10}_{-25}	250^{+10}_{-25}	

vacuum pumps were located beneath the balcony for ease in removal of castings and maintenance of the vacuum system. A 50-kw, 440-volt, 3000-cycle motor-generator unit supplied the necessary power for melting. Views of the furnace above and beneath the balcony are shown in Figures 8A and 8B. The major components of the furnace (shown in Figure 9) consisted of the following: the furnace base, cold trap, pumping system, covers, insulation, induction coil, and quartz tube.

The base of the furnace is a stainless steel box, 18 x 23 in. and 10 in. high, to which is welded a circular flange to permit an O-ring vacuum sealing of the mold well underneath the base. Similarly, a circular flange is welded at the top for the support and sealing of the quartz tube.

The quartz tube, sealed to the furnace base by a flat, silicone rubber gasket, was nominally 13 in. OD by 36 in. long with a $\frac{3}{8}$-in. wall thickness. Both ends of the tube were ground perpendicular to the axis of the tube to remove defects and to insure sealing under vacuum. The top of the tube was sealed by a water-cooled cover, again using a flat, silicone rubber gasket. The cover was fitted with a rotating sight glass and a compression-ring fixture for the pull rod.

The quartz tube was insulated by tongue-and-grooved, high-density stabilized zirconia bricks, measuring 4 x $4\frac{1}{2}$ in. and 1 in. thick, with a radius of $8\frac{1}{2}$ in. These bricks were supported by a stainless steel ring which was an integral part of the top flange of the furnace base. The inside diameter of the insulation was 10 in. The insulation was sufficient to keep the quartz tube below any color temperature.

Power from the high-frequency generator was induced into the furnace via a coil surrounding the quartz tube. Problems associated with power loss from corona discharge and/or direct arcing were eliminated by using an exterior coil rather than one inside the vacuum chamber.

The proper match between generator and load (crucible and charge) was obtained with a coil of 12 turns, which gave the necessary ampere-turns for inducing the necessary generator power into the load. The 12-turn coil had a 14-in. ID, leaving a $\frac{1}{2}$-in. gap between the coil and quartz tube, and was 15 in. high for distribution of flux over the crucible and crucible cover. The coil consisted of two parallel strands of $\frac{1}{2}$ in. OD x $\frac{3}{8}$ in. ID copper tubing, silver brazed together at intervals along its length. With this double strand winding, the turn spacing was approximately $\frac{1}{4}$ in. The two strands were connected directly to a copper bus bar and water cooled, the water being introduced through copper terminal blocks silver brazed to each end of the coil.

Coil dimensions and turn spacing were maintained by six Micarta bars spaced 60° apart, to which each turn of the coil was bolted by a silver-brazed stud. Two of the Micarta bars extended to the balcony floor and supported the coil.

FIGURE 8A. View of 13 in. Quartz Tube, Vacuum Induction Furnace from Balcony Floor

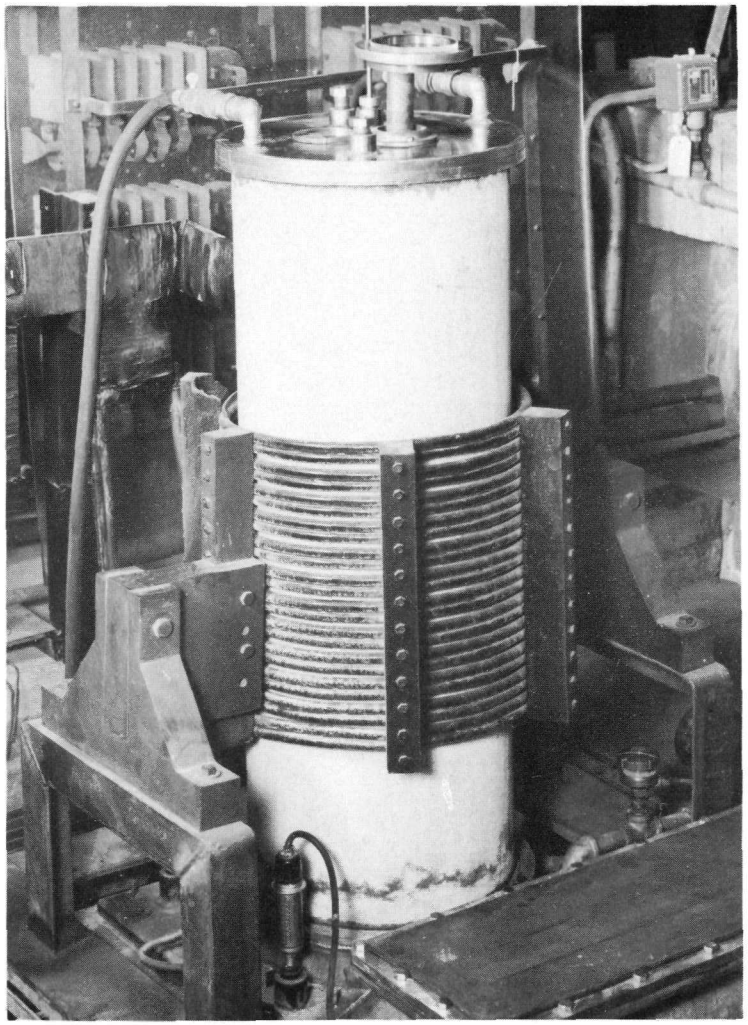

106-4176

FIGURE 8B. Subfloor Mold Removal Area and Vacuum System for 13 in. Quartz Tube Furnace

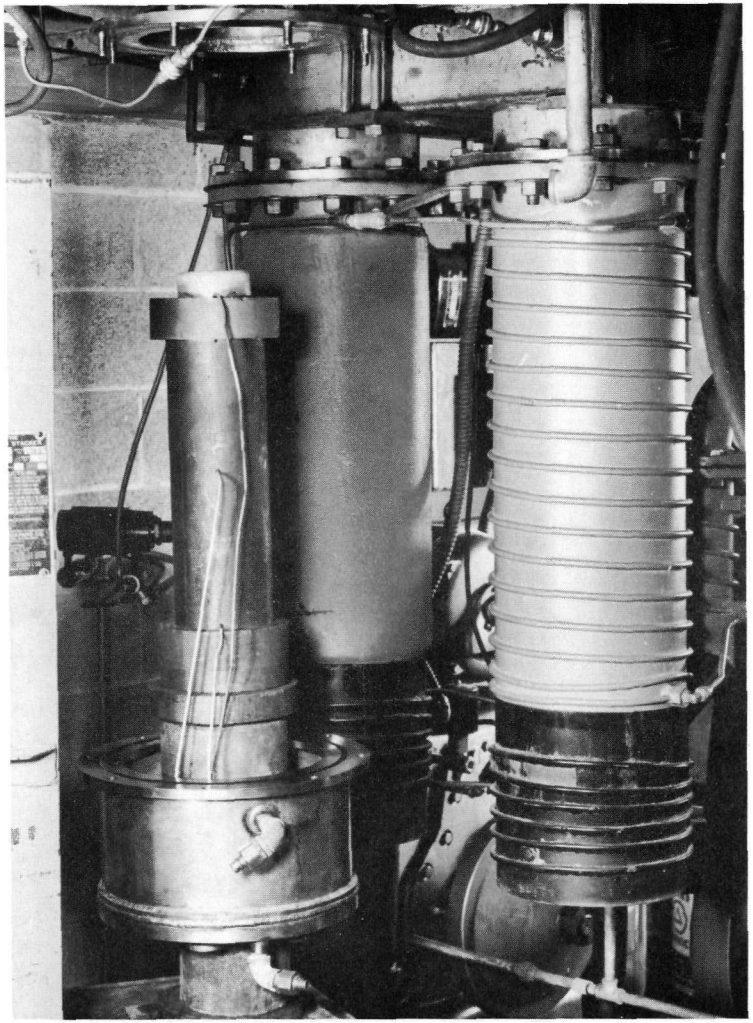

106-4179

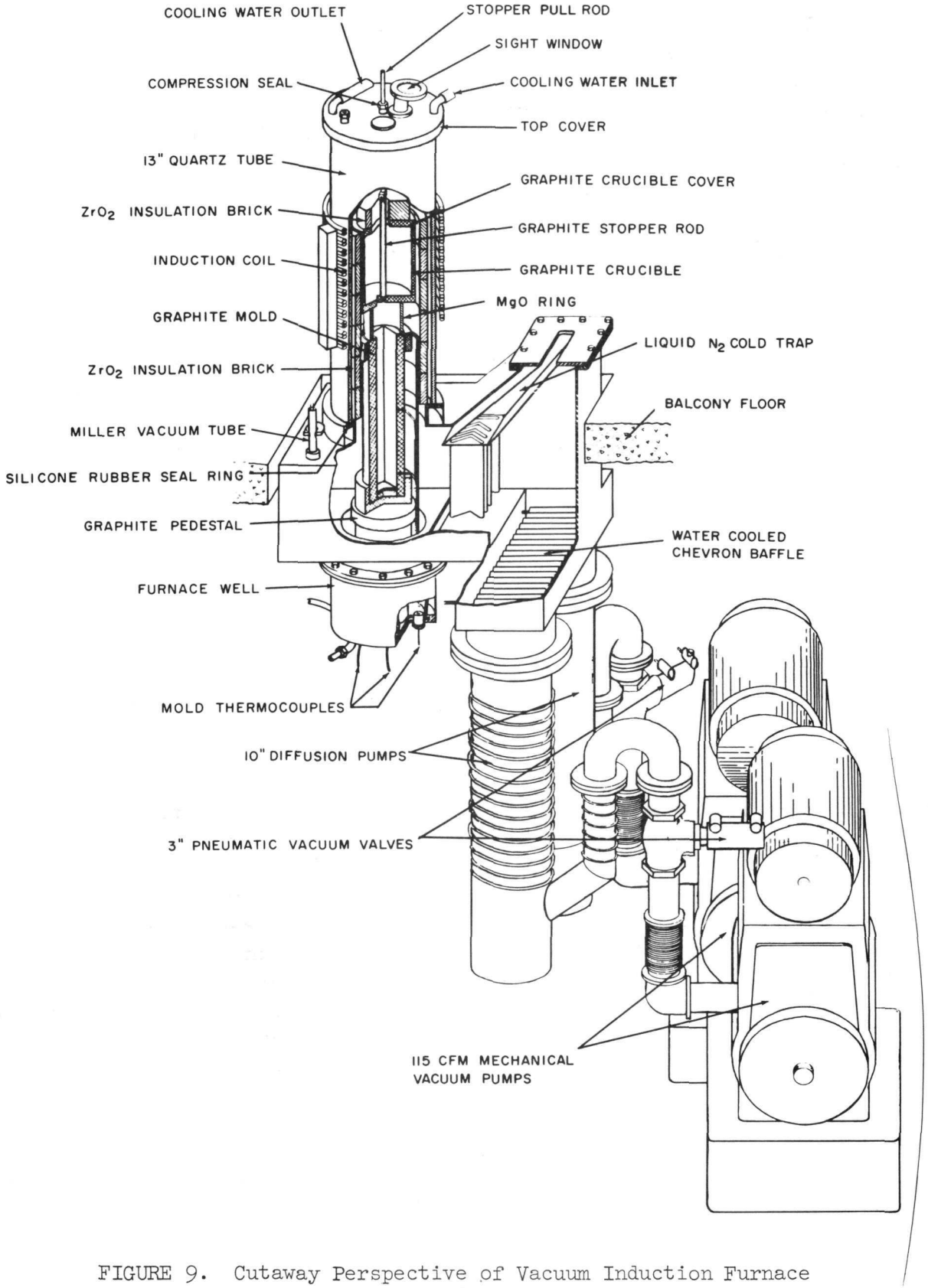

FIGURE 9. Cutaway Perspective of Vacuum Induction Furnace for Core Alloy Production

A four-strand, cluster-connected, positive-negative-positive-negative cable transmitted power from the generator to a condenser bank from which the power was fed to the coil by water-cooled bus bars having a $\frac{1}{4}$ x 4-in. cross section. The variable capacitance condenser bank permitted balancing of the inductive load with capacitance to obtain a leading power factor as near unity as possible. Of the 160 microfarads of total capacitance, 64 microfarads could be switched in or out of the circuit in seven steps ranging from 4 to 32 microfarads by contactors controlled by push buttons. Operation of the high-frequency motor generator and the capacitor bank was carried out at a control panel located on the balcony.

The furnace pumping system was capable of maintaining a vacuum of 0.3 micron during melting and 0.03 micron during periods of superheat. The vacuum system consisted of two identical and independent pumping units connected in parallel. Each unit consisted of a 10-in. National Research Corporation H-10 diffusion pump, type 01-1011, having a pumping speed of 3000 cfm at a pressure of 0.5 micron; and a Stokes Microvac pump, model 212, having a pumping speed of 115 cfm. Both units were employed during each heat.

Control of the pumping system was carried out at the furnace control panel located on the balcony. The panel contained switches for starting and stopping the mechanical and diffusion pumps, opening and closing of the vacuum valves, and adjusting the power input to the diffusion pump heaters. Meters for measuring the power input to the heaters and the furnace vacuum were also located on the control panel. Immediately below the control panel were a series of valves controlling the flow of cooling water to the various parts of the furnace (flanges, cover, induction coil, etc.) and the pumping system. Interlocks and relays protected the pumping system against errors in starting sequence or water failure.

The furnace was equipped with chevron-type water-cooled baffles to impede the diffusion of pump oil into the furnace. These baffles were located directly above the high-vacuum openings of the diffusion pumps and between the pumps and the cold trap. The cold trap, located between the furnace and the diffusion pumps, was situated to one side of the furnace in a stainless steel housing and was filled with liquid nitrogen through an opening located in front of the quartz tube on the balcony floor.

The 3-in. vacuum valve was a pneumatically operated, electrically controlled, bellows sealed, globe-type valve and was located between the mechanical pump and diffusion pump to maintain the vacuum in the furnace after pump shutdown.

Crucible and Mold Arrangement

The crucible and mold were arranged in the furnace as illustrated in Figure 9. To arrange for the proper height of the mold and crucible, it was necessary to use a pedestal, 11½ in. high, which rested on the bottom of the mold well. This well contained four compression-type fittings through which the three mold thermocouples were led from the furnace. The graphite mold rested directly on top of the pedestal and, when the mold well was bolted and sealed to the furnace base, the top of the mold was 2 in. beneath the induction coil. With the mold in this position, the proper thermal gradient was developed for production of sound castings.

A magnesia ring, 4½ in. OD, 4 in. high, and of ¼-in. wall thickness, was placed on the top of the mold; this had a threefold purpose: (1) to serve as a hot top for molten metal, (2) to support the crucible and charge, and (3) to restrict heat flow to the mold. Because of the insulating property of MgO, heat transfer to the mold by conduction was practically eliminated. Similarly, heating of the mold by radiation was lessened due to the space afforded by the 4-in. MgO ring. The heating of the mold, therefore, was by radiation and possibly by induction, since the mold was sufficiently close to the coil to be contained in its generated flux pattern.

A ¾ in. thick graphite cover was placed on top of the crucible, and the cover, in turn, was insulated by 2½ in. of zirconia brick. With the stopper rod placed in the crucible pouring hole, the furnace cover seated on the quartz tube, and the pull rod connected to the stopper rod and passing through the compression fitting in the cover, the furnace arrangement was complete.

Mechanics of Melting

Despite the wide differences in melting points and densities between aluminum and the alloy additions, no great problem in alloying or recovery of metal was encountered. The aluminum, the base metal and by far the greatest volume of metal in the charge, melted first (about 660°C) and completely covered the solid uranium and nickel, the latter elements remaining at the bottom of the crucible due to their differences in densities from that of the liquid. Alloying was then accomplished by holding at a sufficiently high temperature to insure dissolution. This dissolution was abetted by agitation generated through induction stirring and physical movement of the small nickel shot as it went into solution.

To aid dissolution, all melting and casting was done in vacuum. Surface oxidation of the alloying constituents was thereby retarded considerably by decreasing the activity of the atmospheric contaminants. Melting normally took place in vacuums of less than one micron.

Another factor beneficial in retarding uranium oxidation at elevated temperature was the rapidity with which the aluminum melted. On the average, the aluminum was completely molten within 23 min of initial power input. The uranium, because of its greater density, was completely submerged and wetted by the molten aluminum, thereby promoting solid-liquid diffusion.

The ability of aluminum to reduce the oxides of uranium also aided in dissolving the uranium. Any surface oxidation of uranium would be reduced by aluminum and thereby expose pure uranium to the molten aluminum. While the degree of surface oxidation of the uranium was reduced to a minimum due to the machining done on the uranium casting and the short time at elevated temperatures before melting of the aluminum, the reducing ability of aluminum decreased the time necessary for dissolution of uranium.

Melting and Casting

Preparation for a melt cycle began with placing the graphite mold on the pedestal in the mold well. The three thermocouples were then inserted in the mold, led through the compression fittings in the well, and tested for continuity. Once inserted through the compression fittings, the thermocouples did not have to be removed in subsequent melts, barring a failure of a thermocouple.

The mold well was raised up to the furnace base by a manually operated, portable lift truck and bolted to the bottom flange on the base. The lines carrying cooling water to the mold well were fitted, and the thermocouples connected to Leeds and Northrup potentiometers.

With the exception of obtaining mold temperatures, all remaining operations were performed on the balcony. With the mold and well in place, the MgO ring was carefully centered on the top of the mold. After the coated crucible was placed on the MgO ring and the stopper rod inserted in the pouring hole, the charge was carefully loaded into the crucible and the graphite cover and zirconia insulating brick put in place. The tantalum pull rod, passing through the compression fitting in the furnace cover, was connected to the stopper rod and the cover carefully lowered onto the quartz tube. Connection of the cooling water lines to the furnace cover completed the operations prior to evacuation and melting.

The melt cycle was initiated by starting the mechanical pumps and opening the vacuum valves. When the furance vacuum reached 90 microns or less, the diffusion pumps were put into operation. The cold trap was filled with liquid nitrogen when the vacuum reached 10 microns and, when the vacuum was less than one micron, the power was applied.

All 68 castings were produced using the same melt cycle, this cycle being necessary to achieve the critical mold temperatures as discussed earlier. A summary of a typical heat log is given in Table II; and melting and casting data for individual heats are presented in Table III. From the beginning of melting until melting was complete, the power was reduced to decrease bubbling and splashing, which caused metal loss through the crucible cover opening.

Metal temperatures during heating were measured by means of a Leeds and Northrup optical pyrometer sighted on the surface of the metal. Radiant heat from the heavily insulated crucible cover resulted in the top surface of the molten metal being the hottest portion of the pool. The recorded temperatures, therefore, were the maximum attained by the metal.

After pouring and sufficient cooling of the casting, the mold was removed by opening and unloading the furnace in the reverse order of loading. The mold was disassembled and the casting removed and conditioned. Figure 10 shows a mold partially disassembled and the casting still in place. The interior walls of the mold were lightly sanded prior to reuse, and the crucible and stopper rod were scraped free of metal and recoated with the duplex ceramic wash. Damaged stopper rod tips were repaired by machining.

Casting Evaluation

Upon completion of a weight balance on the casting process for U^{235} accountability, each casting was radiographed to determine if porosity or segregation was present.

All radiographs were made using a General Electric OX-250KV industrial X-ray unit. The casting was positioned 48 in. from the source and a 230-sec exposure time was used with 250 kv and 10 ma. Type AA film with 0.010-in. lead sheets on either side of the film was used for all exposures.

After developing, each radiograph was evaluated to determine the presence and extent of porosity or segregation. All acceptable castings showed a slight amount of segregation at the juncture between the hot top and the 2 x 4-in. cross section. This segregation later showed up as a definite pattern in the rolled plate and will be discussed further in evaluating rolled material.

Prior to the use of premelted uranium in the charge, castings exhibited severe porosity, as seen in Figure 11, a reproduction of the X-ray radiographs of a defective casting (A7) and an acceptable casting. The defective casting was cut at the dotted line and the section polished and photographed. The cross section is shown in Figure 12, and the severe porosity present is typical of the initial castings made with biscuit uranium.

TABLE II. Log of a Typical Virgin Heat

Heat No.: A21

Composition:
17.46 w/o highly enriched U
2.00 w/o nickel shot
0.41 w/o iron
Balance Aluminum

Date: 3/18/58

Charge	Wt, gm
M388 Alloy (Al-1 w/o Ni)	6627.43
Premelted Uranium (B16F-241)	1420.78
Nickel Shot	90.20
	8138.41

Crucible

Graphite: 7 in. ID x 8 in. OD x 10 in.
$\frac{3}{8}$-in. dia pouring hole

Wash: 2 coats $MgO-ZrO_2$; 1 coat ThO_2.

Mold

Graphite: 2 x 4 x 19 in.

Wash: None

Melting Data

Time	Power, kw	Optical Temp, °C	Vacuum, μ	Remarks and Condition of Melt
9:25	38		0.08	Power on; start of heat.
9:38	12		1.8	Melting rapidly; power lowered reduce bubbling.
9:45	34		0.31	Power raised to bring melt to 1050°C; slight bubbling
9:54	8	1059	0.82	Melt at 1050°C. Reduce power and hold $\frac{1}{2}$ hr at 1050°C.
10:24	10	1053	0.15	Power raised to bring melt to 1075°C. Melt quiet.
10:30	10	1072	0.13	Melt at 1075°C. Hold $\frac{1}{2}$ hr.
11:00	0	1076	0.20	Power off, cool melt to 925°C.
11:13	6.8	923	0.08	Power on, hold 15 min at 925°C.
11:28	6.8	927	0.06 (before pouring)	Poured.

Weight of Casting: 8086.55 gm

Weight of Skull: 51.86 gm

Recovery: 99.4%

Surface Condition: Good; minor cold shuts on one side.

TABLE III

Summary of Melting and Casting Data and Weight of Billet for Rolling

Melt No.	Charge Weight (gm)	Melt Cycle Time		Vacuum, μ		Pouring Temp (°C)	Casting Weight (gm)	Conditioned Billet Weight (gm)
		hr	min	Minimum	At Pour			
A-1	7807.18	1	55	1.1	1.1	922	7715.67	- *
A-2	7798.66	1	58	0.50	0.52	920	7561.31	- *
A-3	7920.84	1	55	1.1	1.1	927	7745.96	- *
A-4	7893.77	2	26	0.05	0.05	918	7747.12	- *
A-5	8097.32	1	57	0.07	0.08	922	7894.57	- *
A-6	8100.47	3	22	0.03	0.04	927	7881.73	- *
A-7	8101.89	1	53	0.05	0.05	922	7956.61	- *
A-8	8109.17	1	58	0.20	0.46	942	7934.57	- *
A-9	8129.98	1	53	0.24	0.86	935	7970.50	7204.31
A-10	8130.37	1	58	0.11	0.11	938	7922.65	7185.50
A-11	8051.38	2	12	0.02	0.06	927	7969.82	7185.87
A-12	8139.65	2	05	0.03	0.04	927	8079.82	7212.11
A-13	8137.51	2	06	0.02	0.04	927	7922.00	7184.36
A-14	8140.90	2	25	0.02	0.12	925	7841.21	7159.68
A-15	8142.88	2	02	0.04	0.04	928	7954.56	7208.65
A-16	8247.84	1	56	0.04	0.06	932	8149.15	7186.14
A-17	8141.42	1	52	0.05	0.05	923	8088.58	7188.46
A-18	8144.86	2	26	0.04	0.06	933	7890.72	7110.29
A-19	8142.99	2	10	0.03	0.08	926	8081.91	7202.92
A-20	8144.55	1	55	0.06	0.06	932	8070.80	7139.90
A-21	8138.42	2	03	0.06	0.06	927	8086.55	7176.65
A-22	8142.04	2	01	0.06	0.10	928	8038.20	7190.73
A-23	8137.90	2	09	0.05	0.05	926	8040.11	7202.93
A-24	8140.04	2	03	0.07	0.07	923	8068.10	7192.52
A-25	8142.60	2	04	0.07	0.07	929	8082.01	7198.34
A-26	8136.23	1	55	0.07	0.07	935	8081.66	7195.26
A-27	8141.30	2	02	0.08	0.08	928	7957.06	7178.98
A-28	8137.57	1	51	0.10	0.10	923	8047.88	7178.37
A-29	8179.93	1	58	0.08	0.08	925	8064.23	7316.55
A-30	8138.33	1	56	0.04	0.06	928	7975.73	7308.88
A-31	8199.11	1	58	0.06	0.12	928	8143.27	7325.21
A-32	8202.02	2	-	0.07	0.07	925	8154.02	7314.68
A-33	8213.90	1	52	0.08	0.08	924	8173.89	7311.76
A-34	8197.83	1	55	0.08	0.08	925	8141.24	7349.86
A-35	8201.42	2	03	0.07	0.07	930	8121.75	7350.19
A-36	8206.65	1	56	0.04	0.10	926	8135.79	7339.05
A-37	8199.21	1	59	0.10	0.10	927	8118.04	7350.34
A-38	8200.81	1	58	0.09	0.10	928	8040.35	7322.81
A-39	8200.95	2	05	0.12	0.12	925	7992.24	7318.24
A-40	8211.36	2	07	0.08	0.08	925	8039.77	7312.20
A-41	8200.17	2	02	0.14	0.14	927	8043.38	7306.28
A-42	8231.57	2	01	0.10	0.14	928	8145.31	7313.65
A-43	8299.49	2	07	0.07	0.10	928	8138.81	- *
A-44	8578.12	1	54	0.02	0.30	933	8463.21	7330.06
A-45	8225.75	1	45	0.12	0.40	925	8146.25	7346.44
A-46	8308.79	1	50	0.12	0.24	927	8153.54	7341.06
A-47	8401.75	2	05	0.02	0.16	932	8195.12	7285.80
A-48	8290.94	1	52	0.03	0.18	928	8152.32	7340.02
A-49	8394.85	2	02	0.02	0.76	932	8271.38	7365.07
A-50	8431.13	2	10	0.03	0.16	927	8334.55	7374.18
A-51	8417.52	2	02	0.04	0.90	930	8303.81	7372.79
A-52	8384.85	2	03	0.02	0.30	925	8148.82	7368.48
A-53	8380.47	2	07	0.02	1.8	929	8255.72	7355.43
A-54	8477.67	2	-	0.06	0.40	927	8359.35	7360.47
A-55	8355.06	1	55	0.04	0.40	930	8254.49	7355.24
A-56	8461.12	2	-	0.12	0.90	923	8337.15	7356.55
A-57	8366.69	1	54	0.08	1.2	928	8218.13	7336.63
A-58	8585.81	2	02	0.04	3.3	928	8158.72	7306.13
A-59	8451.59	2	-	0.27	0.88	927	8267.26	7297.77
A-60	8433.49	1	49	0.18	0.85	930	8317.03	7329.70
A-61	8400.22	2	07	0.05	2.2	927	8279.27	7352.55
A-62	8462.58	1	56	0.27	0.90	927	8257.39	7348.11
A-63	8401.96	1	59	0.04	0.96	927	8270.49	7330.15
A-64	8202.13	1	55	0.02	0.40	927	8039.73	7332.59
A-65	8229.50	1	52	0.06	0.58	928	8118.98	7299.45
A-66	8288.84	2	01	0.06	0.34	927	8242.55	7338.36
A-67	8275.57	1	59	0.04	0.96	927	8149.81	7309.43
A-68	8446.46	2	05	0.04	0.60	925	8362.01	7320.24

*Casting was porous and was remelted.

FIGURE 10. Partially Disassembled Mold with Casting in Place

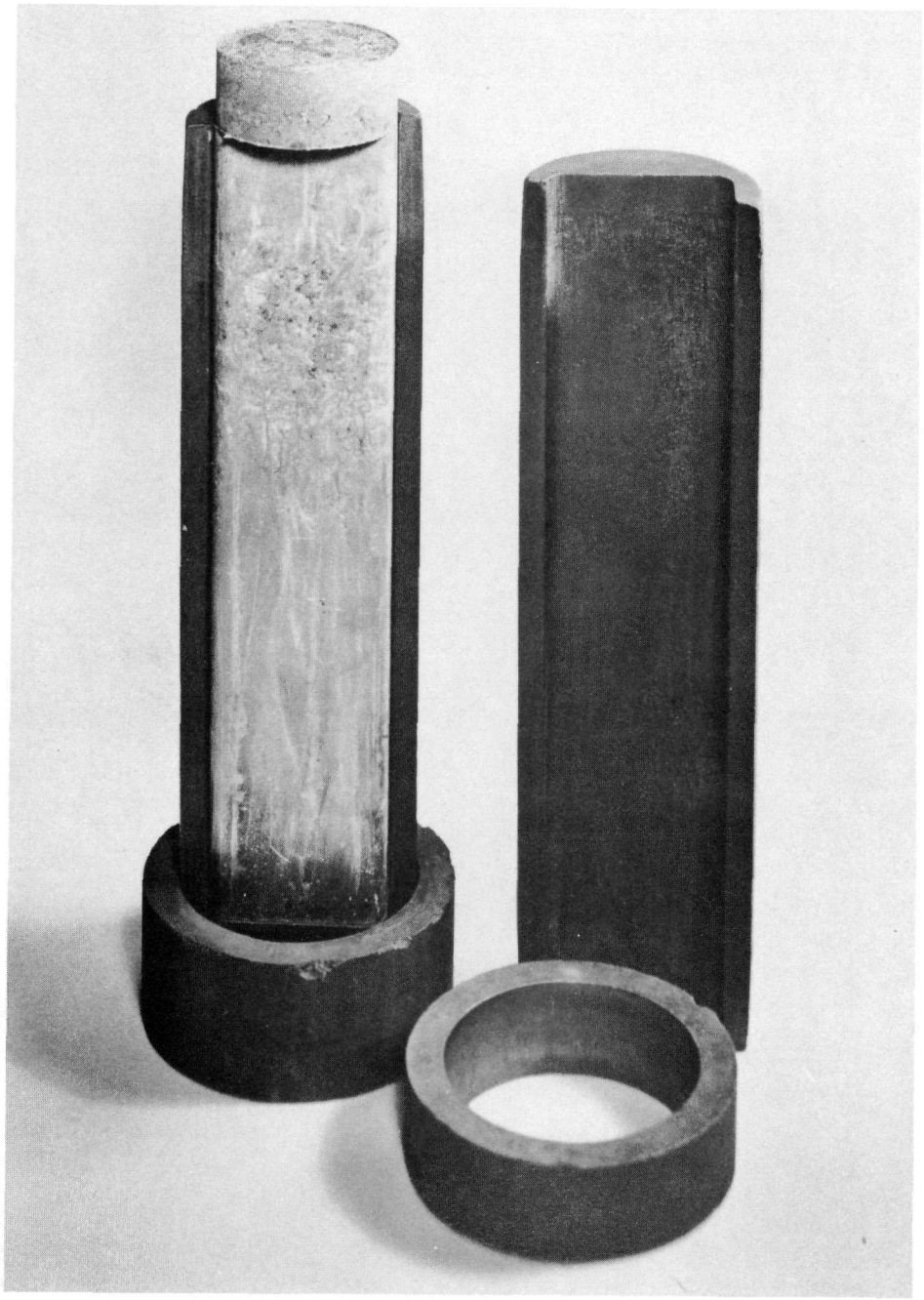

106-4185-A

While the cast surfaces were good in general, all castings showed a slight amount of cold shuts at the corners in the middle of the casting. These were not serious and were removed before rolling of the casting.

FIGURE 11. Print of X-ray Radiographs of Defective and Acceptable Castings

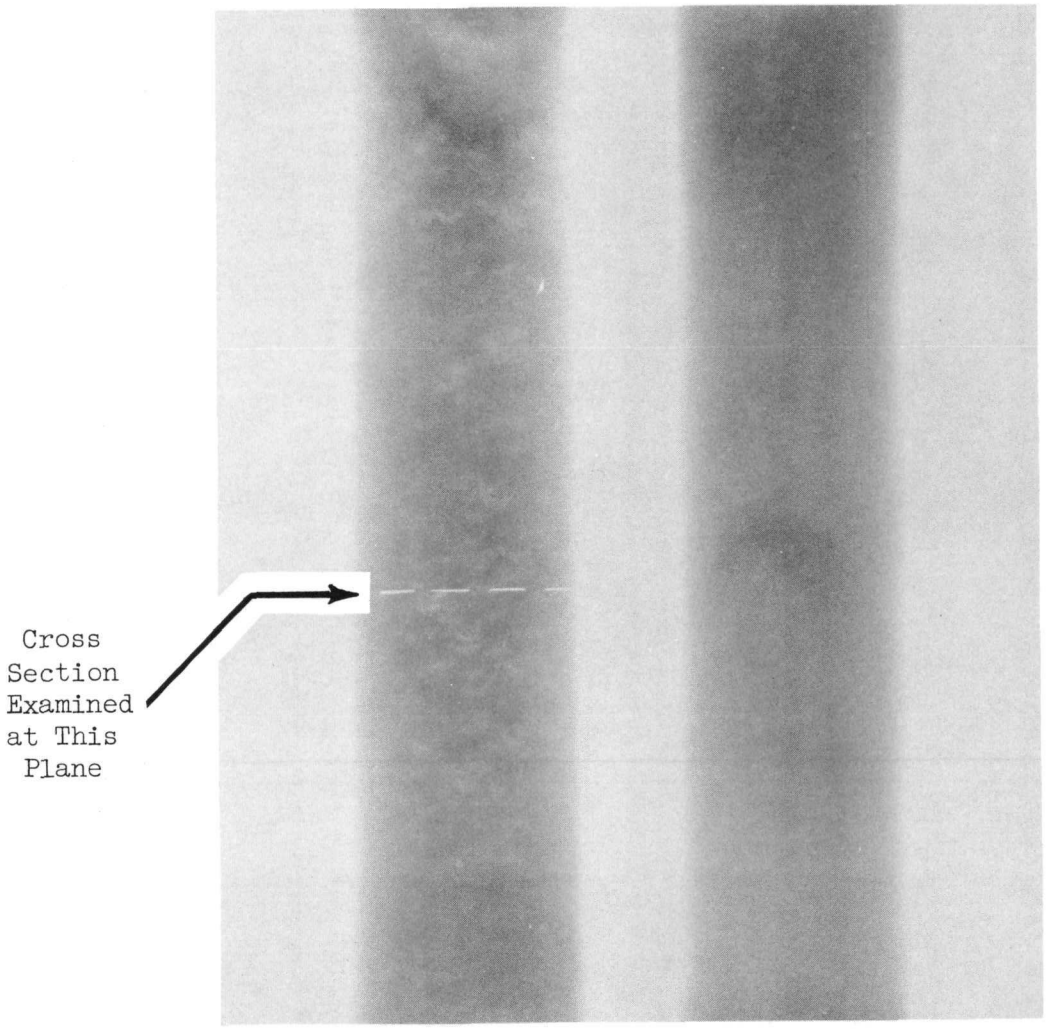

106-4192 Defective Acceptable 1/4X

FIGURE 12. As-polished Cross Section of Defective Casting

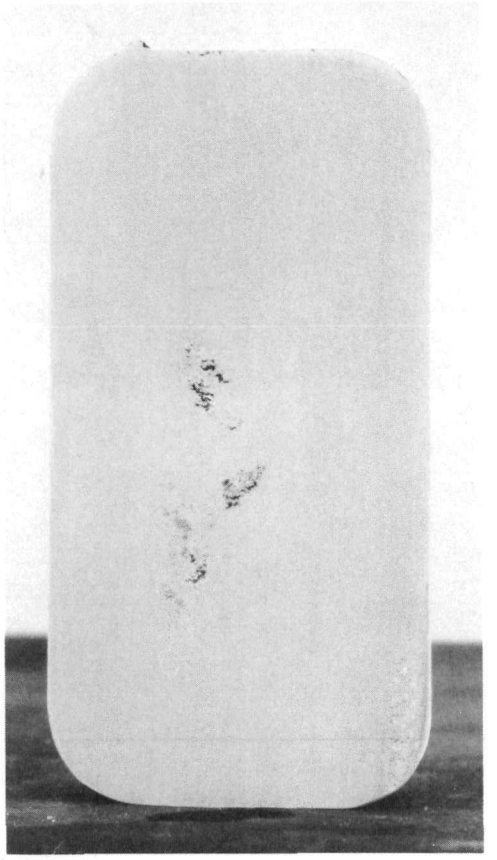

24058 1X

Sectioned at Dotted Line on Defective Casting Shown in Fig. 11.

CONDITIONING OF CASTINGS

It was necessary to condition the castings prior to the rolling operation. This conditioning consisted of removing the hot top, machining the base of the casting, and removing the fins and cold shuts on the casting surface.

Figure 13 illustrates the removal of the hot top on a Steptoe-Western shaper using a high-speed, tool steel parting tool. Water was used as a lubricant to prevent buildup on the tool point and galling of the machined surface. The total weight of the hot tops removed constituted 8.26% of the total casting weight. This material was salvaged by remelting.

A light cut was taken across the bottom end of the casting to remove the rough surface and possible contamination from the graphite bottom plug in the mold.

The small fins running along the length of the casting and resulting from liquid metal filling and solidifying in the seams of the split mold were removed by filing. Similarly, any cold shuts present on the cast surface were removed by filing to prevent lapping in later rolling operations. Figure 14 shows a casting after removal from the mold and a casting that has been conditioned suitably for rolling.

While specifications called for analytical sampling to be made on rolled material, samples were taken from the top and bottom of the first nine physically acceptable castings. These analyses were to serve as rough estimates of composition and to reject castings far out of specified chemistry limits before rolling the plate and punching cores. This sampling was discontinued when the high degree of segregation at the top sample location was discovered. It was felt that the analytical results were not representative and were invalid for the casting as a whole.

FABRICATION OF CORE BLANKS

Development

Initially, the 2 x 4 x 18$\frac{1}{2}$-in. conditioned billets were to be hot rolled at 550°C to a 0.200-in. thick strip. Rolling was to be done in the long direction, and the billet reheated for ten minutes between each pass. A two-hour preheat was used, and the roll speed set at 120 ft/min.

Experimental castings rolled in this manner developed serious edge cracking after approximately 50-60% reduction in area. Crack penetration was so severe that there was insufficient material from which to punch 3.316-in. wide core blanks. Had such a roll schedule proved feasible, the finished strip would have been approximately 0.200 in. thick x 4 in. wide x 185 in. long.

FIGURE 13. Removing Hot Top from Casting

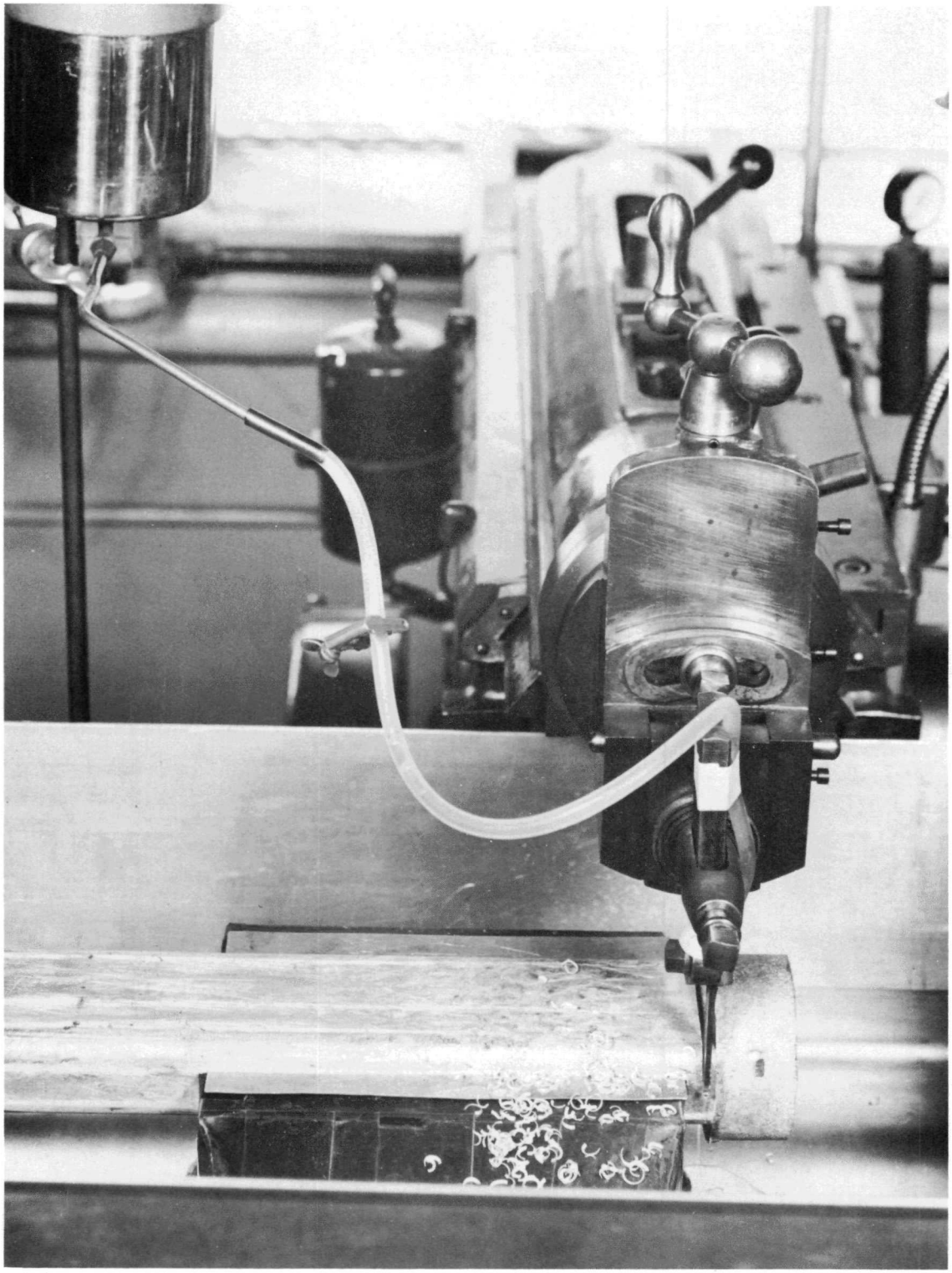

106-4175

FIGURE 14. Castings As Removed from Mold (bottom) and after Conditioning (top)

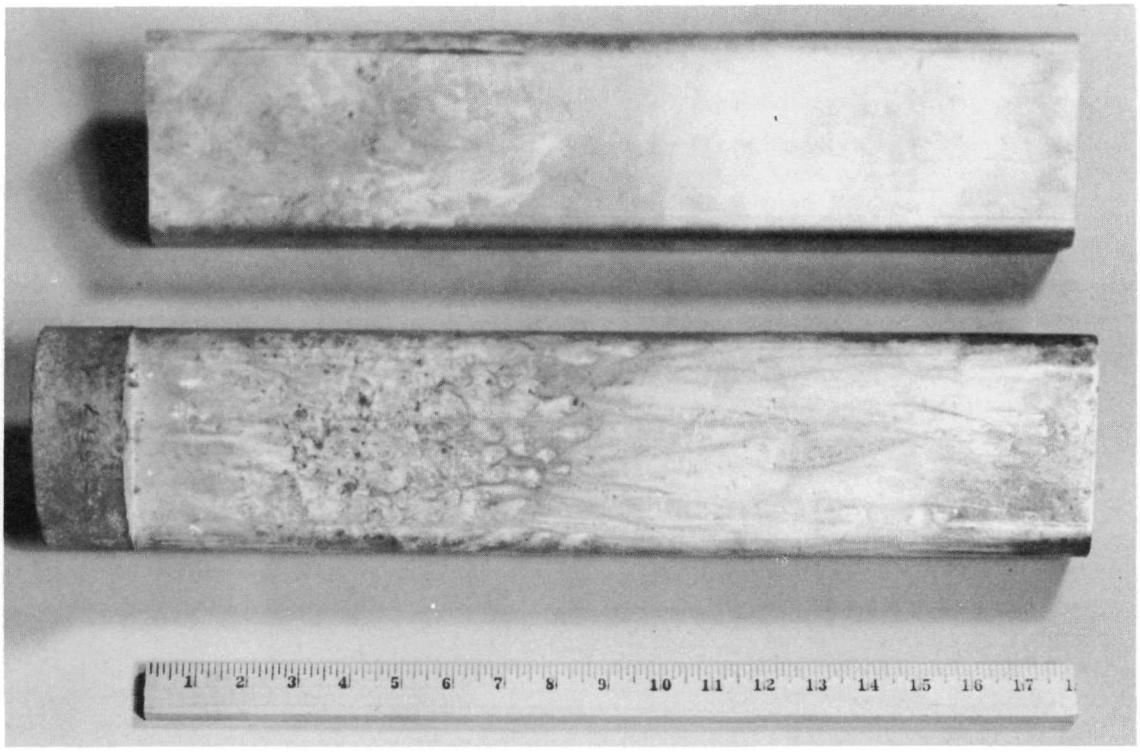

106-4181

As it was felt that the Al-U eutectic temperature of 640°C prevented a sufficient increase in rolling temperature to eliminate the edge cracking, the billets were cross-rolled to an 8-in. width and long-rolled to the final thickness. The finished plate, 0.200 in. x approx. 8 in. x approx. $92\frac{1}{2}$ in. long, would permit two rows of core blanks punched parallel to the final rolling direction or a single row of core blanks punched in the transverse direction.

Cross-rolling to an 8-in. width was tried and, while edge cracking was considerably reduced, it was still severe enough to cast doubts as to the reproducibility of results from such a schedule. The first acceptable billet (A9) was rolled in this manner. It was hot rolled to a thickness of 0.205 in. and cold finished to 0.201 in. The width varied from 8 to $8\frac{1}{8}$ in. and the length was approximately $86\frac{3}{4}$ in. (initial billet length was $18\frac{3}{16}$ in.). Serious edge cracking occurred at the top and bottom edges where the uranium content varied due to segregation in the billet.

Billet Rolling

On the basis of the first billet, a new rolling schedule, as shown in Table IV, was established. The rolling temperature was increased to 580°C,

TABLE IV. Roll Schedule for Processing ALPR Billets

Stock: ALPR Billets, 2 x 4 x $18\frac{1}{2}$ in.
Rolling Mill: 17 x 24 in., 2-high
Roll Speed: 120 ft/min
Heating Medium: Air
Rolling Temperature: 580°C
Preheat Time: 2 hr
Reheat Time: 10 min/pass

Pass No.	Roll Parting (in.)	Draft (in.)	Reduction (%)	Plate Thickness (in.)	Remarks
1	1.815	0.185	9.3	1.815	Cross rolling (hot)
2	1.665	0.150	8.3	-	
3	1.513	0.152	9.1	1.512	
4	1.364	0.149	9.8	-	
5	1.213	0.151	11.1	1.212	
6	1.062	0.151	12.4	-	
7	0.932	0.130	12.2	0.930	
8	0.801	0.131	14.1	-	
9	0.670	0.131	16.4	0.668	
10	0.541	0.129	19.3	0.540	
11	0.430	0.111	20.5	0.428	Long rolling (hot)
12	0.324	0.106	24.6	-	
13	0.230	0.094	29.0	0.227	
14	0.221	0.009	3.9	0.216-0.217	Cold rolling
15	0.210	0.011	5.0	0.208-0.209	
16	0.206	0.004	1.9	0.203-0.204	
17	0.206	0.000	0	0.201-0.202	
18	0.206	0.000	0	0.198-0.201	

Rolled Dimensions

Billet Condition	Width (in.)		Thickness (in.)		Length (in.)
	max	min	max	min	
Cross rolled	$14\frac{1}{8}$	$12\frac{1}{4}$	0.540	Average	$18\frac{1}{2}$
Hot rolled	$14\frac{1}{8}$	$12\frac{11}{16}$	0.226	0.225	$44\frac{1}{16}$
Cold rolled	$14\frac{3}{16}$	$12\frac{5}{8}$	0.201	0.198	$49\frac{11}{16}$

and the billet cross rolled to a minimum width of 12 in. before long rolling to the final thickness of 0.200 in. Hot rolling, still utilizing a two-hour preheat and a ten-minute reheating between passes, was employed down to a 0.230-in. thickness from which the plate was cold rolled to size. This schedule proved very satisfactory and, while slight edge cracking still occurred, crack penetration did not extend into material to be sheared for core punching.

After ten passes, the billet reached the minimum 12-in. width and had a maximum width of $14\frac{1}{4}$ in. The minimum width occurred at the ends of the plate, where heat loss and subsequent lateral restraint are greatest and resistance to plastic deformation the highest. At this point, plate thickness was approximately 0.540 in. A typical cross-rolled plate is illustrated in Figure 15.

FIGURE 15. Typical Cross-rolled Billet

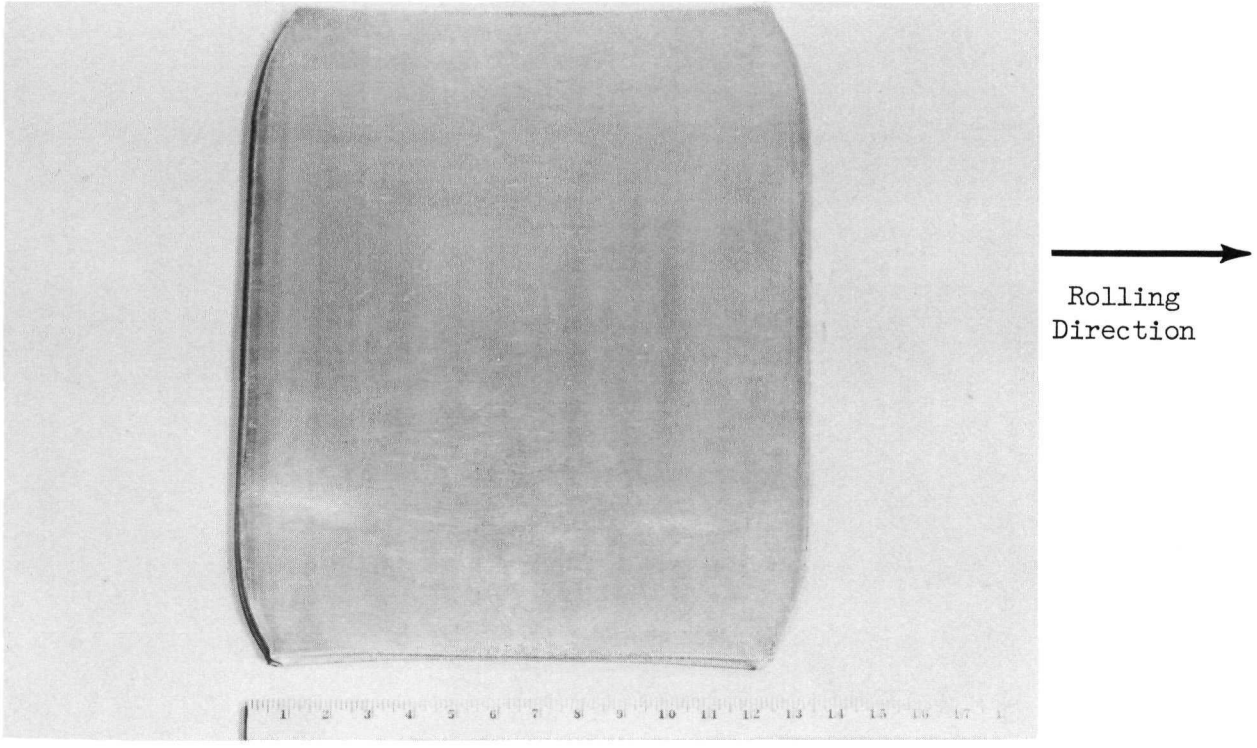

106-4183-A

Following reheating, the cross-rolled billet was long rolled down to 0.225-0.228-in. thickness in four passes, the length of the hot-rolled plates varying from $42\frac{3}{4}$ to $44\frac{1}{2}$ in. The plates were then cold rolled to a nominal 0.200-in. thickness in four passes. Finished plate lengths varied from $48\frac{1}{4}$ to $51\frac{3}{4}$ in., depending on the initial length of the conditioned billet before rolling. A finished plate is shown in Figure 16 together with a cross-rolled plate and a conditioned billet.

Hot and cold rolling was performed on a 17 x 24-in., two-high rolling mill. The mill was equipped with 5-in. diameter, $\frac{1}{4}$-in. pitch Acme thread screws driven by a 5-hp, shunt-wound DC motor through a gear reduction and worm and pinion. The roll bearings were Timken, 4-row, tapered roller type and mounted in cast steel chocks. The top roll and chocks were balanced by means of four hydraulic oil cylinders mounted two in each bottom chock. The rolls were chill-cast, alloy cast iron and were ground without crown.

FIGURE 16. Stages of Billet Fabrication: Conditioned Billet, Cross-rolled Billet, and Finished Rolled Plate (bottom to top)

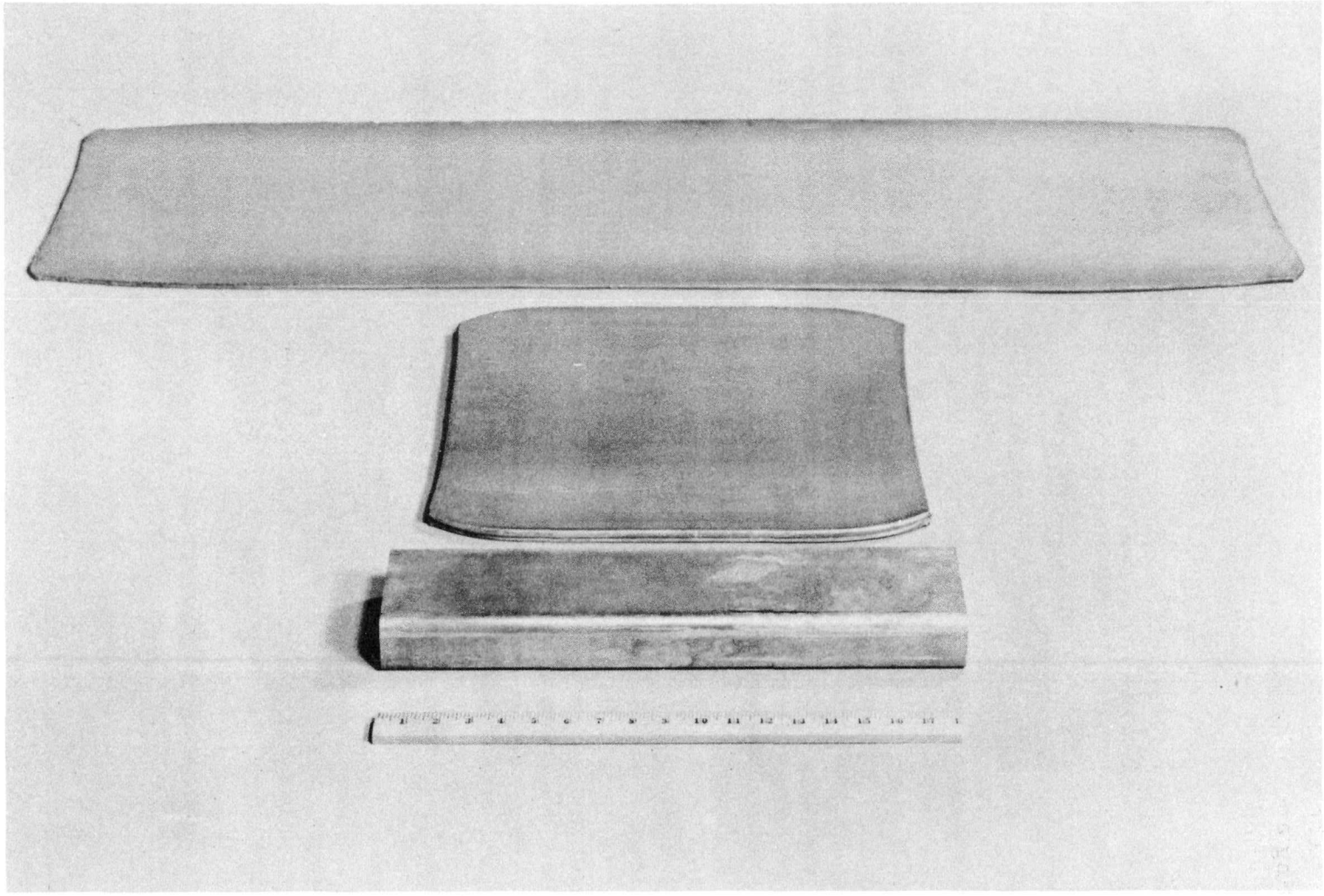

106-4184-A

The rolls were driven by a 150/200-hp, shunt-wound DC motor through a combination drive and pinion stand with a 15.56 to 1 reduction.

The mill was equipped with power-driven roller tables to assist in handling and to assure uniform conveyance of material. A more detailed description of the rolling mill and its associated equipment can be found in ANL-5629.[3]

The preheating of billets for rolling and reheating between passes was done in two electric, Hevi-Duty furnaces, one being rated at 36 kw with an 18 in. wide x 72 in. long hearth, and the second rated at 150 kw with a 38 in. wide x 109 in. hearth with three-zone heating. Billets were placed upright along their longitudinal length in the furnace to facilitate handling and to accommodate three or four at a time. Stainless steel racks were placed in the furnaces to maintain the plates in an upright position.

A palm oil lubricant was used during rolling to prevent pickup of aluminum or aluminum oxide on the roll surface, which would result in poor surface quality. The rolls were wiped with a sponge bearing the lubricant after each pass.

During cross rolling, a stainless steel sheet was placed upon the roller tables to prevent gouging and scratching of the billet by the edges of the tables. The heated billet was placed adjacent to the mill rolls, the rolls engaged, and the billet fed into the mill with tongs having a steel strip welded across the open jaws. One operator transported billets to and from the mill by means of tongs.

Long rolling was carried out in the same manner, with the exception of the sheets on the roll tables. These were removed and the motor-driven feed and runout tables - synchronized to the roll speed - were used to feed and remove the plates from the rolls.

After the last hot pass, the plates were air cooled and then cold finished to size. When the plates reached the nominal thickness of 0.200 in., they were measured for thickness, width, and length.

Rippling or warping occurring in the plate during cold rolling was removed by roll straightening done on a 9-roll Waterbury-Farrel roller leveler with a $15\frac{1}{2}$-in. roll face. Figure 17 shows a plate being roll straightened.

Preparation of Core Strips

After straightening, the plates were marked for shearing strips from which to punch core blanks. The strips were 4 in. wide to allow approximately $\frac{5}{16}$ in. on either side of a core blank in the punching operation. The length of the strip was determined by the maximum number of core blanks

FIGURE 17. Straightening of Rolled Plate in Roller Leveler

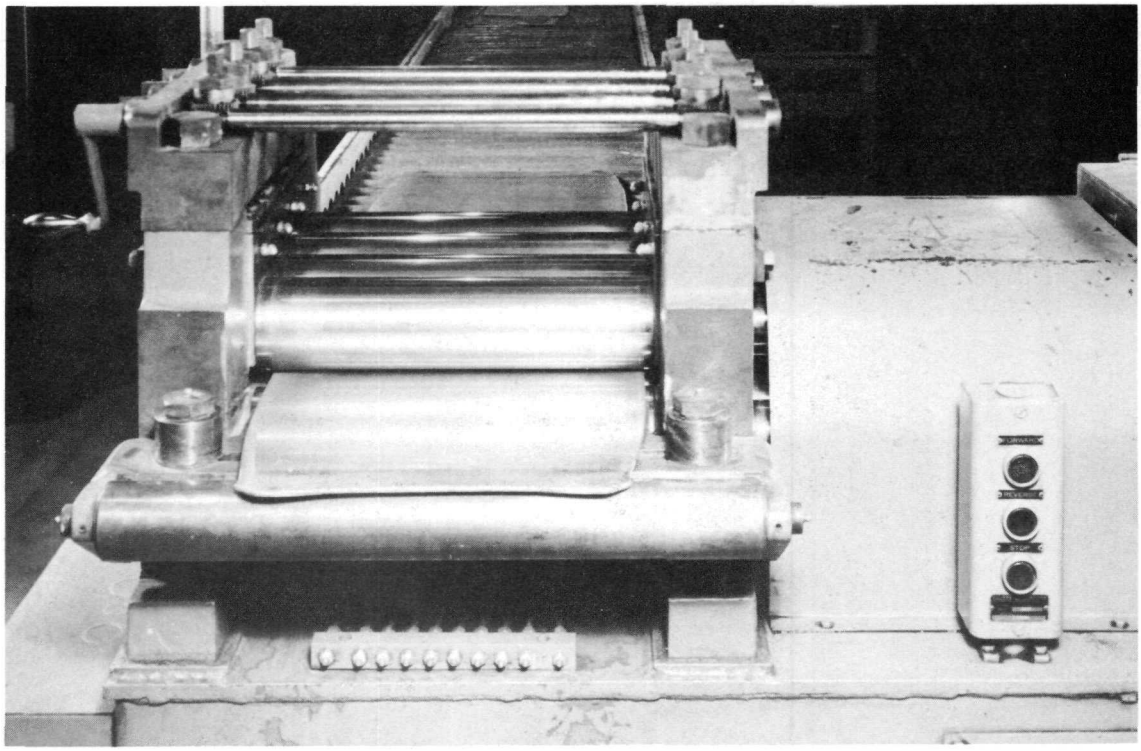

106-4178

(core blank length being $6\frac{7}{8}$ in.) that could be punched from the length of the plate with an allowance of $\frac{1}{4}$ in. between core blanks for punching stock. The plate length of the initial billets was sufficient to punch a row of six core blanks (a required strip length of 43 in.), but $\frac{1}{2}$ to $1\frac{1}{2}$ in. short of the 50-in. minimum length necessary to punch seven core blanks. These plates were marked and sheared to provide three strips, each of which would yield six core blanks, and a fourth 4-in. wide strip cut in the transverse plate direction to realize an additional core blank and a total of 19 punched core blanks. The strip yielding the single core blank was taken from either the top or bottom section of the plate, depending on which area was the best. Plates of length greater than 50 in. were sheared into three strips 4 in. wide x 50 in. long, and yielded a total of 21 core blanks on punching.

Records were kept of the shearing and punching operation to insure identification of punched core blanks and shearing scrap with respect to location in the rolled plate. The scrap generated in shearing was used as remelt stock for later castings.

Shearing was done on a Cincinnati shear rated for $\frac{1}{2}$-in. mild steel. The shearing table was covered with paper to prevent scratching of the plate during positioning and shearing. In addition, a pad of paper was placed on top of the plate to prevent marking or indenting of the plate by the hold-down pads during the shearing cycle. The operation is shown in Figure 18, and a typical sheared plate in Figure 19. The latter shows the three strips 4 in. wide x 50 in. long, and the trimmed sides and ends which later were remelted.

FIGURE 18. Shearing of Rolled Plate into Strips for Core Blank Punching

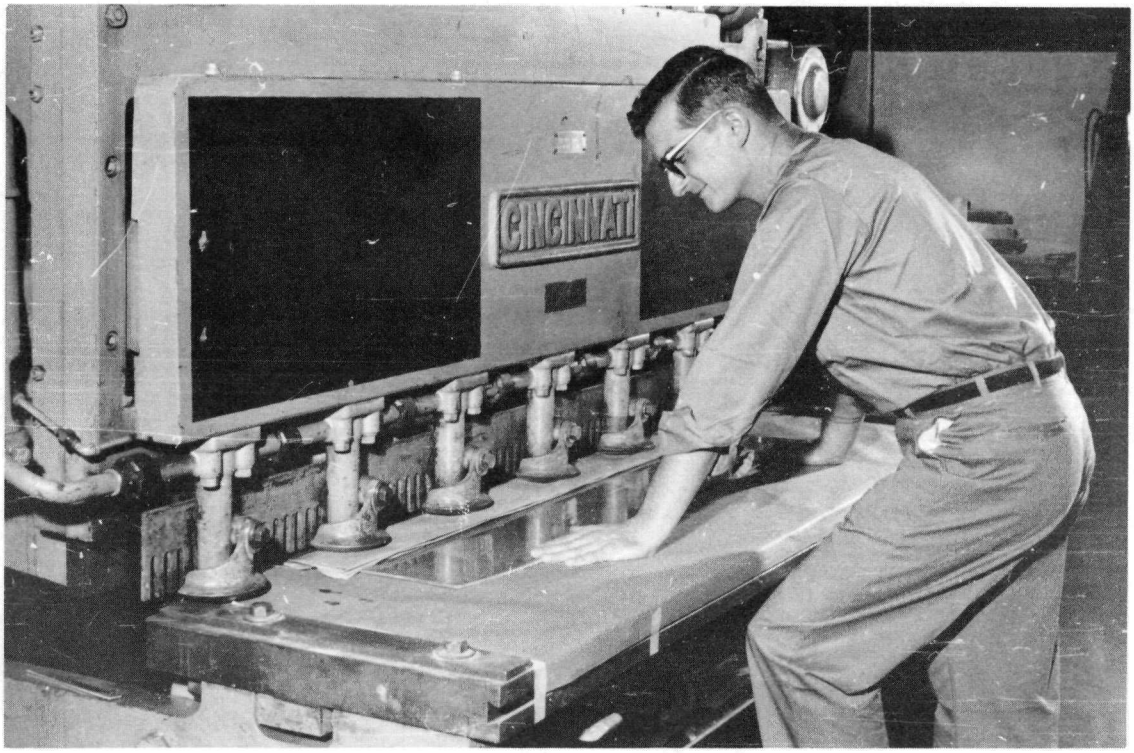

FIGURE 19. Typical Sheared Plate Showing Three Strips for Core Blank Punching and Scrap Sides and Ends

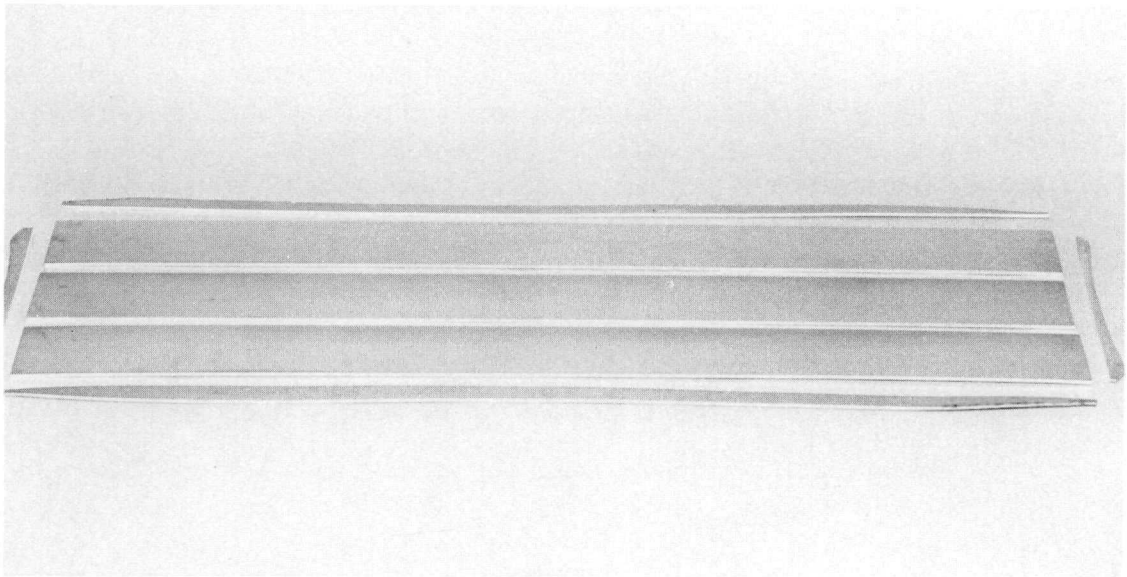

106-4186

Analytical samples were cut from the top and bottom sheared ends for spectrochemical determination of the nickel and iron contents and of the major impurities. The samples were approximately $\frac{3}{4}$ in. square and machined on one side to provide a proper surface for analysis. The analytical results for each plate are reported in Table V.

The sheared strips were wiped with acetone to remove any dirt or grease, and the thickness of the strip measured 1 in. in from both edges at 6-in. intervals. Should the thickness exceed the high limit of 0.201 in., the strip was cold rolled to size and flattened in the roller-leveler.

It was found that the roll surfaces had a worn spot resulting in a non-uniform thickness of the plate. For the most part, this nonuniformity occurred in the center strip; consequently, it was necessary to reroll many center strips from plates fabricated before the rolls were reground.

Prior to punching, the strips were scribed in such a manner as to insure identification of the core blanks and the surrounding material with respect to location in the rolled plate should future evaluation of core material require this information.

Punching and Preparation of Core Blanks

Core blanks were punched on a 25-ton Loshbough-Jordan punch press driven by a 2-hp motor. A tool steel die plate on a steel backup plate and a tool steel punch were used. The die cavity measured 3.316 in. wide x 6.875 in. long, with a 0.002-in. clearance between the punch and die. Hard rubber pads were located inside the die cavity to eject the punched core blank from the die when the punch returned to its raised position.

The core strip was placed in the press and positioned against the guide pins by one operator while a second man operated the foot trip lever. After a core blank was punched, it was removed with a pair of tongs and the strip advanced into position for punching the next core blank. An overall view of the press and the two operators ready to punch a core blank is shown in Figure 20A; a closeup view of the die with the strip in position for punching is shown in Figure 20B. Figure 21 shows seven punched core blanks and the remaining lattice with two unpunched strips.

The lattice remaining from the strip after punching was used for analytical samples for uranium analysis by wet chemistry. While various patterns of sampling were tried in order to obtain sufficient analytical data for determining the U^{235} content per core blank, no sampling plan was found which would give sufficiently reliable data with minimum sampling. Consequently, the U^{235} content was based on a nondestructive, gamma-emission counting method to be discussed in detail in a later section of the report. Samples for uranium determination by wet chemistry were taken, however,

TABLE V Composition of Rolled Plates for ALPR Fuel Plate Cores

Melt No.	Alloy Content										Impurities					
	Uranium, w/o					Isotopic % U^{235}	Nickel, w/o(1)		Iron, w/o(1)		Minor Elements, %(2,6)					
	1	2	3	4	Avg(3) for plate		Top	Bottom	Top	Bottom	Cr	Cu	K	Mg	Mn	Pb
A-9	20.36	(4)	18.28	(4)	17.50	93.20	1.58	1.56	0.37	0.42	L0.05	0.3	L0.1	L0.01	0.01	L0.01
A-10	20.74	(4)	19.12	(4)	17.46	93.20	1.73	1.82	0.37	0.42	L0.05	0.3	L0.1	L0.01	0.01	0.04
A-11	18.18	(4)	17.58	(4)	17.52	93.20	1.83	1.58	0.40	0.39	L0.05	0.3	L0.1	L0.01	0.01	0.01
A-12	18.96	(4)	18.46	(4)	17.46	93.20	1.64	1.77	0.40	0.39	L0.05	0.4	L0.1	L0.01	0.01	L0.01
A-13	17.62	(4)	17.92	(4)	17.50	93.21	1.75	1.82	0.38	0.46	L0.05	0.4	L0.1	L0.01	0.01	0.04
A-14	17.51	(4)	17.48	(4)	17.42	93.20	1.87	2.04	0.38	0.44	L0.05	0.3	L0.1	L0.01	0.01	0.04
A-15	18.08	18.66	17.50	17.50	17.47	93.20	1.72	1.80	0.41	0.42	L0.05	0.3	L0.1	L0.01	0.01	L0.01
A-16	18.08	18.52	17.39	17.34	17.47	93.20	1.63	1.70	0.43	0.43	L0.05	0.3	L0.1	L0.01	0.01	L0.01
A-17	18.36	18.69	17.66	17.70	17.64	93.20	1.62	1.68	0.38	0.38	L0.05	0.3	L0.1	L0.01	0.01	0.03
A-18	19.30	19.57	17.80	17.60	17.57	93.20	1.68	1.57	0.39	0.37	L0.05	0.3	L0.1	L0.01	0.01	0.02
A-19	17.51	17.54	17.58	17.46	17.56	93.20	1.53	1.98	0.34	0.42	L0.05	0.4	L0.1	L0.01	0.01	0.01
A-20	17.98	17.25	17.84	19.86	17.67	93.26	1.75	1.85	0.41	0.43	L0.05	0.4	L0.1	L0.01	0.01	L0.01
A-21	18.20	17.96	17.27	17.50	17.68	93.26	1.72	1.80	0.38	0.42	L0.05	0.3	L0.1	L0.01	0.01	L0.01
A-22	16.86	16.86	17.47	17.54	17.68	93.26	1.58	1.50	0.39	0.39	L0.05	0.3	L0.1	L0.01	0.01	L0.01
A-23	17.59	17.40	17.11	17.24	17.64	93.20	1.73	1.83	0.39	0.43	L0.05	0.3	L0.1	L0.01	0.01	L0.01
A-24	17.15	17.16	17.39	17.31	17.80	93.20	1.44	1.69	0.37	0.40	L0.05	0.3	L0.1	L0.01	0.01	L0.01
A-25	17.22	20.02	18.18	18.06	17.62	93.20	(5)	1.80	(5)	0.40	L0.05	0.3	L0.1	L0.01	0.01	L0.01
A-26	17.08	17.13	17.62	17.19	17.58	93.20	1.74	1.82	0.36	0.44	L0.05	0.3	L0.1	L0.01	0.01	0.03
A-27	17.36	16.98	17.37	17.04	17.47	93.30	1.80	1.60	0.43	0.41	L0.05	0.3	L0.1	L0.01	0.01	0.05
A-28	17.28	17.59	17.29	17.51	17.48	93.30	1.65	1.87	0.46	0.48	L0.05	0.3	L0.1	L0.01	0.01	0.03
A-29	16.80	17.09	17.05	17.17	17.47	93.30	1.75	1.80	0.40	0.43	L0.05	0.3	L0.1	L0.01	0.01	L0.01
A-30	16.82	16.87	17.18	16.20	17.45	93.30	1.45	1.58	0.36	0.39	L0.05	0.4	L0.1	L0.01	0.01	0.02
A-31	17.23	17.20	17.50	17.58	17.52	93.24	1.73	1.95	0.45	0.51	L0.05	0.08	L0.1	L0.01	0.01	0.02
A-32	17.30	17.57	17.58	17.62	17.62	93.24	1.78	2.08	0.51	0.54	L0.05	0.02	L0.1	L0.01	0.01	L0.01
A-33	17.31	17.30	17.21	17.38	17.53	93.24	1.82	1.88	0.52	0.53	L0.05	0.01	L0.1	0.01	0.03	L0.01
A-34	17.53	17.86	20.02	17.72	17.72	93.24	(5)	1.80	(5)	0.49	L0.05	0.03	L0.1	L0.01	0.03	L0.01
A-35	18.88	18.49	17.63	17.64	17.60	93.28	(5)	1.58	(5)	0.40	L0.05	0.01	L0.1	0.01	0.03	L0.01
A-36	19.07	17.96	17.98	17.29	17.66	93.28	(5)	1.63	(5)	0.44	L0.05	0.01	L0.1	L0.01	0.03	L0.01
A-37	18.24	17.54	17.57	17.76	17.64	93.28	1.60	1.54	0.41	0.42	L0.05	0.01	L0.1	L0.01	0.03	L0.01
A-38	17.00	16.89	17.37	17.22	17.58	93.28	1.58	1.65	0.39	0.44	L0.05	0.01	L0.1	L0.01	0.03	L0.01
A-39	17.22	17.30	17.31	17.37	17.33	93.20	1.60	1.62	0.43	0.45	L0.05	0.01	L0.1	L0.01	0.01	L0.01
A-40	17.04	16.85	17.05	17.05	17.23	93.20	1.62	1.65	0.40	0.42	L0.05	0.01	L0.1	L0.01	0.01	0.08
A-41	16.67	16.83	16.80	17.05	17.15	93.20	1.63	1.53	0.38	0.39	L0.05	0.03	L0.1	0.03	0.01	0.05
A-42	17.46	17.38	17.26	17.25	17.26	93.20	1.62	1.63	0.39	0.40	L0.05	0.01	L0.1	0.01	0.01	0.01
A-43	-----	-----	-----	-----	-----	-----	----	-Remelted --		----	-----	----	----	-----	----	-----
A-44	17.14	17.12	17.19	17.42	17.54	93.20	1.73	2.00	0.15	0.18	0.1	0.2	0.3	0.3	0.2	0.03
A-45	17.35	17.02	17.57	17.81	17.68	93.21	1.55	1.58	0.37	0.38	0.5	0.2	L0.1	0.2	0.08	0.02
A-46	17.06	17.41	17.50	17.59	17.42	93.20	2.00	1.75	0.46	0.43	0.02	0.01	L0.1	L0.01	0.01	L0.01
A-47	17.43	17.03	12.80	17.11	17.47	93.20	1.68	1.82	0.33	0.34	0.1	0.4	L0.1	L0.01	0.03	L0.01
A-48	16.79	17.25	17.22	16.90	17.34	93.23	1.41	1.69	0.26	0.32	0.05	0.2	L0.1	L0.01	0.03	L0.01
A-49	17.51	17.72	17.49	17.58	17.60	93.25	1.43	1.00	0.33	0.31	0.2	0.2	L0.1	0.01	0.03	L0.01
A-50	17.63	17.57	17.41	17.51	17.75	93.24	1.30	1.22	0.30	0.32	0.08	0.2	L0.1	L0.01	0.02	L0.01
A-51	17.43	17.07	16.80	17.56	17.74	93.22	1.30	1.34	0.31	0.33	L0.05	0.2	L0.1	L0.01	0.02	L0.01
A-52	17.45	17.50	17.73	17.68	17.66	93.27	1.73	1.68	0.37	0.42	L0.05	0.2	L0.1	0.01	0.02	L0.01
A-53	17.36	17.24	17.35	17.45	17.35	93.20	1.48	1.57	0.38	0.43	L0.05	0.08	L0.1	L0.01	0.02	L0.01
A-54	17.59	17.66	17.79	17.71	17.64	93.26	1.43	1.68	0.44	0.45	L0.05	0.02	L0.1	0.01	0.02	L0.01
A-55	17.41	17.85	17.41	17.34	17.49	93.21	1.63	1.42	0.44	0.37	L0.05	0.08	L0.1	L0.01	0.02	L0.01
A-56	17.29	17.34	17.21	17.28	17.35	93.20	1.34	1.37	0.32	0.36	L0.05	0.08	L0.1	L0.01	0.02	L0.01
A-57	17.30	17.59	17.32	17.49	17.47	93.24	1.30	1.25	0.34	0.33	L0.05	0.08	L0.1	L0.01	0.02	L0.01
A-58	17.37	16.84	17.12	17.13	17.10	93.24	1.30	1.13	0.33	0.37	L0.05	0.3	L0.01	0.02	0.02	L0.01
A-59	17.15	17.57	17.23	17.15	17.14	93.20	1.25	1.32	0.33	0.31	L0.05	0.3	L0.01	L0.01	0.02	L0.01
A-60	17.33	16.90	17.28	17.55	17.49	93.22	1.28	1.16	0.32	0.32	0.3	0.3	L0.01	L0.01	0.02	L0.01
A-61	17.30	18.12	18.42	17.78	17.68	93.21	1.45	1.20	0.31	0.31	L0.05	0.3	L0.01	L0.01	0.02	L0.01
A-62	17.46	17.35	17.78	17.66	17.60	93.24	1.22	1.22	0.31	0.34	L0.05	0.3	L0.01	L0.01	0.02	0.4
A-63	17.12	17.72	17.66	17.74	17.75	93.23	1.23	1.16	0.30	0.35	L0.05	0.3	L0.01	L0.01	0.02	L0.01
A-64	17.27	16.88	17.44	17.44	17.14	93.28	1.40	1.46	0.40	0.45	0.1	0.3	L0.01	0.02	0.02	L0.01
A-65	16.91	17.36	17.11	17.19	17.18	93.21	1.82	1.65	0.43	0.41	0.05	0.3	L0.01	L0.01	0.02	L0.01
A-66	17.12	17.32	17.68	17.60	17.38	93.22	1.63	1.63	0.52	0.42	L0.05	0.3	L0.01	L0.01	0.02	L0.01
A-67	17.01	17.41	16.95	17.41	17.22	93.22	1.55	1.81	0.35	0.54	L0.05	0.3	L0.01	L0.01	0.02	L0.01
A-68	17.35	17.33	17.58	17.51	17.37	93.26	1.63	1.32	0.41	0.41	L0.05	0.3	L0.01	L0.01	0.02	L0.01

(1) Estimated accuracy is 3% of amount present.
(2) Estimated accuracy is the order of magnitude (factor of ten)
(3) Calculated from individual core U^{235} contents determined by gamma-emission counting.
(4) No sample taken.
(5) High U background interfered with analysis of Ni and Fe.
(6) For all melts.
Ag less than 0.01% with exception of A26 which is 0.03%.
As less than 0.5%.
B less than 0.001%.
Ba, Be, Bi, Li, Na, Sb, Sn contents are L0.01%
Ca, Ti, Zn, P less than 0.1%.
Co less than 0.01% with exception of A51 which is 0.05%.
Si less than 0.2% for melts A9 through A57, less than 0.02% for melts A58 through A68.
Zr less than 0.1% with exception of A45 which is L0.2%.

FIGURE 20A. Punching Core Blanks from Sheared Strips

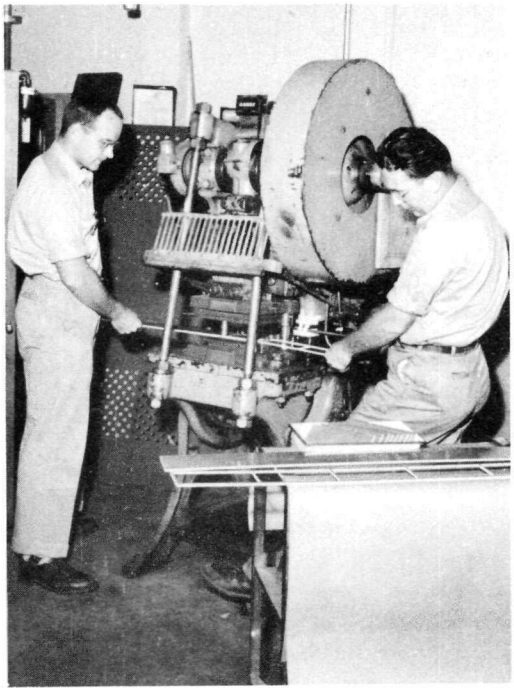

FIGURE 20B. Closeup View of Punching Die with Core Strip in Position

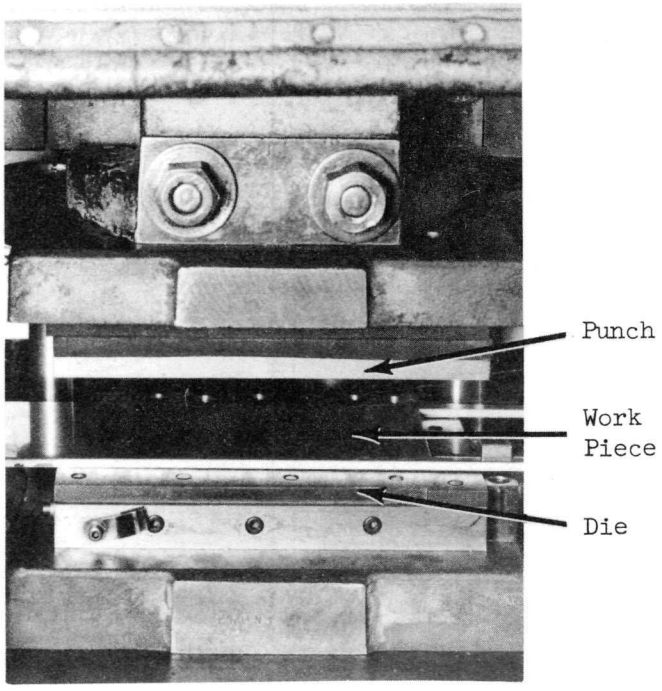

106-4168

FIGURE 21. Core Blanks and Resultant Trellis after Punching Operation

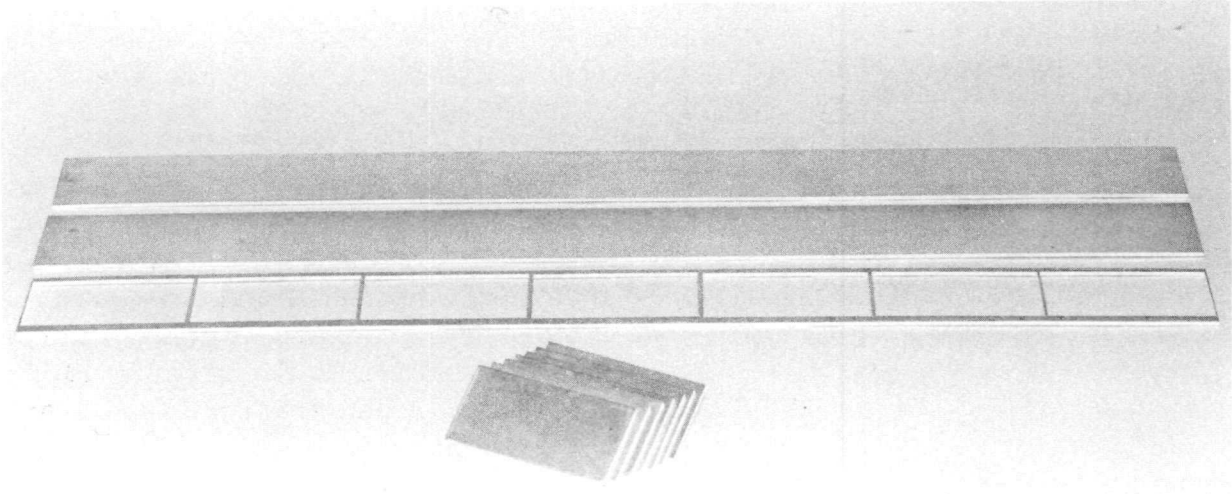

106-4172

to provide a check on the counting method. The samples were taken from the dividing strips between the first two and last two core blanks of the side core strips. These correspond to samples #2, 6, 14, and 18 in Figure 25. The uranium analyses from the samples are given in Table V, in columns numbered 1, 2, 3 and 4, respectively. The "average uranium analyses" of the castings are based on gamma-counting technique.

The remaining lattice material was retained for possible future analytical work, although some material was used for remelt stock in later melts.

The punched core blanks were washed in acetone. This included wire brushing the edges to remove adhering slivers from the punching operation. After the wash, the core blanks were vapor degreased in trichlorethylene in batches of ten. Individual core blank weights were then taken and recorded prior to nondestructive testing of the core blanks.

EVALUATION OF CORE MATERIAL

Nondestructive Core Blank Testing

In addition to chemical analyses of material surrounding the core blanks, the U^{235} content per core blank was determined by the counting of gamma emission from the core blank. The integrity and soundness of each one were evaluated through X-ray radiography and by means of through-transmission ultrasonic scanning. Only a brief description of the tests will be given here as evaluation of the material and the tests will be discussed later. Detail reports on nondestructive testing of ALPR core material and fuel plates are given in ANL-5944[14] and ANL-5951.[15]

Homogeneity of the core material was evaluated through X-ray radiography. Using Type AA film, an exposure of 55 sec at 95 kv, 10 ma, was made with a General Electric OX-250 kv industrial X-ray unit. The core blanks were positioned 48 in. away from the source. A penetrometer with a minimum thickness of 1% of the core blank thickness was used to determine the correct conditions of exposure to insure best radiographic results. Core blanks exhibiting severe segregation in their radiographs were remelted. Figure 22 shows radiographic prints of a good core blank and a reject core blank with serious segregation.

Internal core blank defects such as cracks, inclusions, and segregation were discovered by using a through-transmission ultrasonic technique. The core blanks were supported vertically along one side. Both the core blank and the sending and receiving crystals were submerged in water containing a wetting agent. The sending and receiving crystals were mounted on a yoke such that the two crystals were on opposite sides of the core blank, as seen in Figure 23A. An overall picture of the apparatus and the recording mechanism is shown in Figure 23B.

FIGURE 22. X-ray Radiographs of Acceptable Core Blank (left) and a Core Blank Rejected Due to Major Segregation

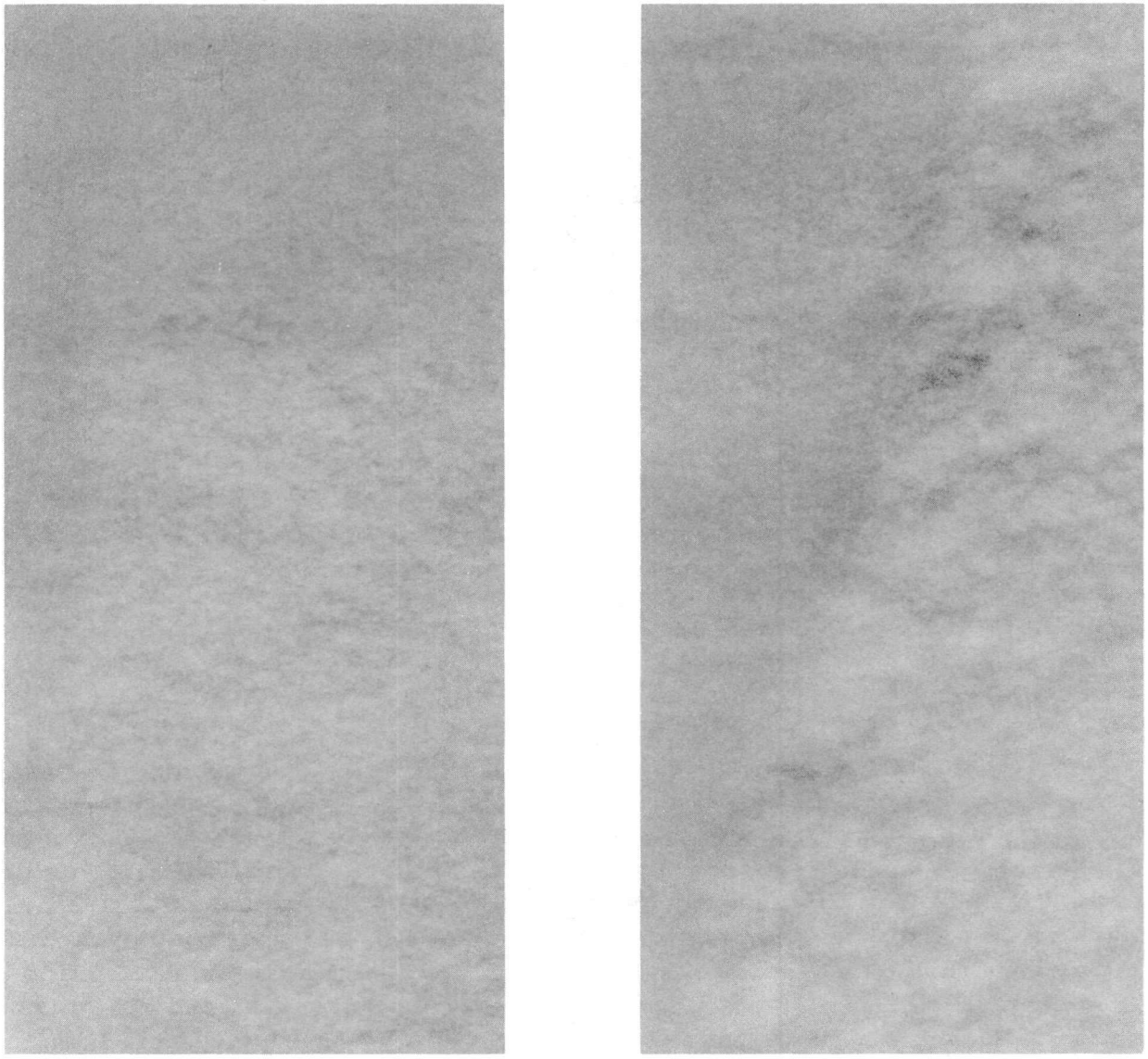

106-4190-A Acceptable Reject

FIGURE 23A. Closeup of Ultrasonic Test Showing Positioned Core Blank and Mechanically Driven Yoke Containing Sending and Receiving Crystals

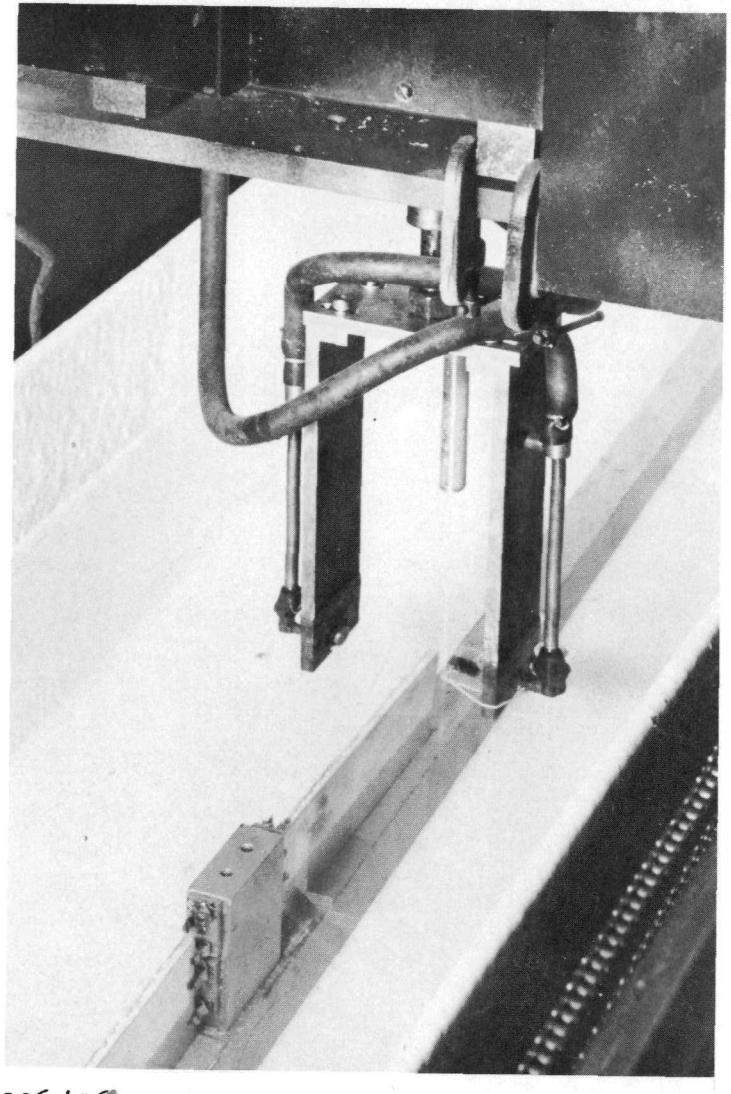

106-4167

FIGURE 23B. Overall View of Ultrasonic Test Equipment with Electrosensitive Paper Recorder in Background

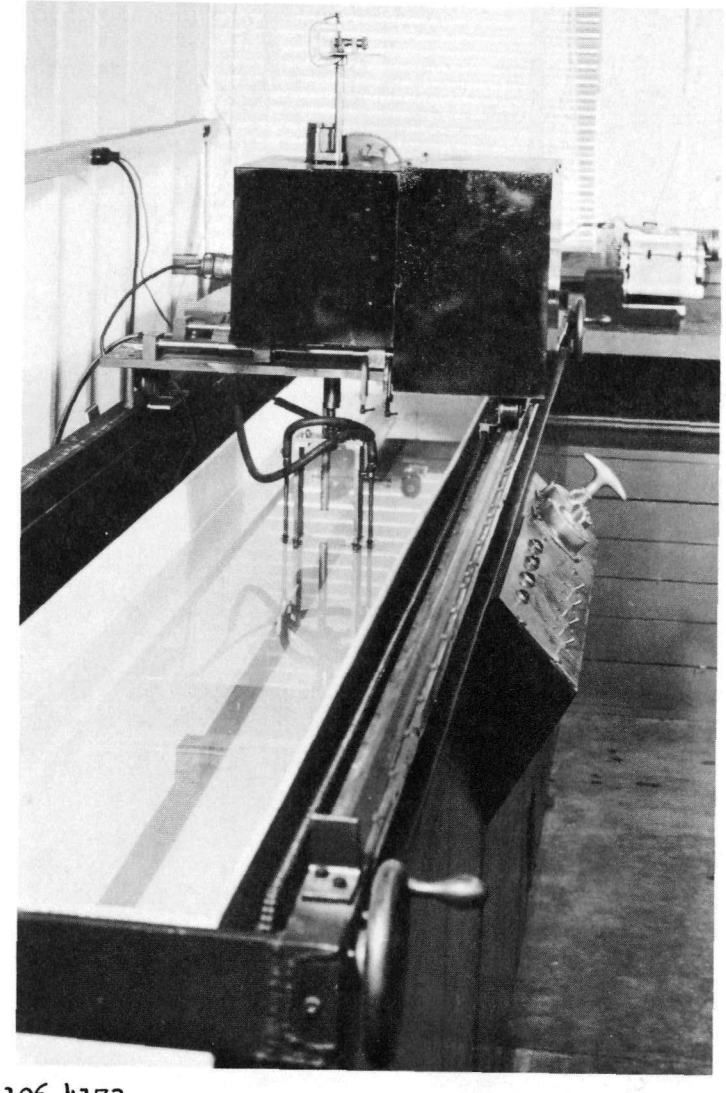

106-4173

The yoke was mechanically driven in such a way that it traveled up and down the core blank width as it traversed the length of the core blank. A two-dimensional plot of the transmitted ultrasonic beam intensity was continuously recorded on electrosensitive paper. A uniform trace density indicated uniform ultrasonic beam transmission and, consequently, no internal defects. A defect would alter the beam transmission and result in a blank area on the paper trace. Figure 24 shows traces from an acceptable core blank and a defective core blank.

FIGURE 24. Permanent Recordings of Reject and Acceptable Core Blanks from Ultrasonic Beam Test As Recorded on Electrosensitive Paper. White areas in left trace indicate defects

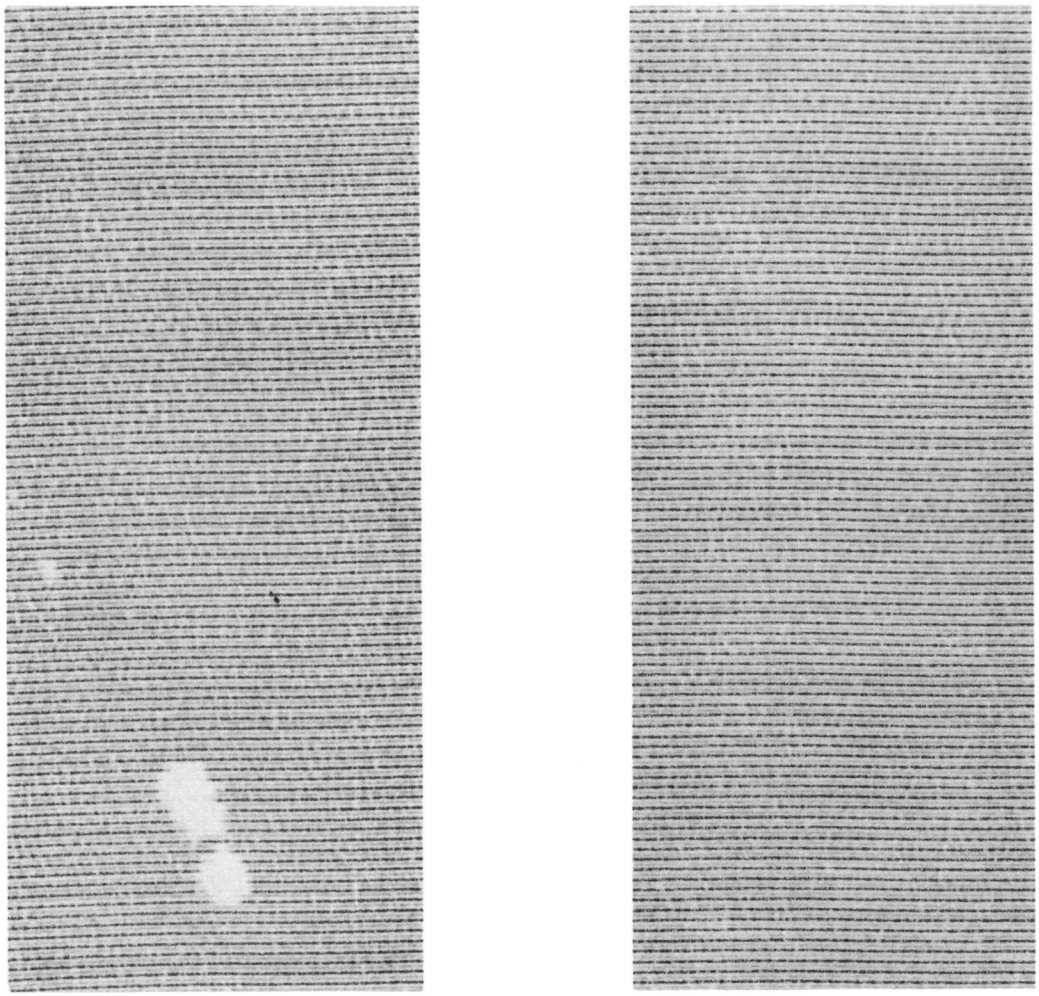

106-4191 Defective Acceptable

The U^{235} content of each core blank was determined by counting the number of gamma emissions in a given period of time. A sodium iodide, thallium-activated scintillation crystal was used to pick up 180-kev emission from a core blank. A five-minute counting period was used and the count rate was approximately 10,000 counts/sec. A standard core blank was counted after every five unknown core blanks to insure reliability of the results. A correlation previously determined between the number of counts and the U^{235} content provided a basis for calculating the unknown U^{235} content of a core blank by the number of counts recorded. The sensitivity of the method could detect a change of 0.1 gm U^{235} in a core blank.(4)

Following nondestructive testing, reject core blanks were remelted while acceptable core blanks were washed in acetone, followed by a rinse in chlorothene, and stored until needed for assembly into compacts for fuel plate fabrication.

Determination of Core Blank U^{235} Content

The core alloy composition was selected such that the fuel plate core blank would contain the specified 39 $\pm$ 1 gm U^{235}. It was necessary to find a method suitable for determining the amount of U^{235} per core blank. Assuming homogeneous material, the simplest method would be a single uranium analysis and an U^{235} isotopic analysis. These, coupled with the weight of the core blank, would determine the U^{235} content.

It became readily apparent from initial wet chemistry uranium analyses that segregation was present in the castings. This segregation was not affected by the fabrication process. An increased number of analyses did not reveal a pattern of segregation that was consistently repeated in other rolled plates.

On plates A19 and A20, samples were taken from lattice material directly adjacent to the top and bottom of each punched core blank. This sampling plan and the resulting uranium analyses are shown in Figure 25. It is readily apparent that the tops of the plates (corresponding to the tops of the castings) were exceptionally high in uranium and that there was a spread of about 2 w/o in the balance of the material. In addition, several core blanks showing variations in uranium content up to 1.8 w/o between top and bottom samples showed no indication of segregation in their X-ray radiographs. On the basis of analytical results and radiography, it was evident that analytical results were valid only for the material analyzed and were not applicable to surrounding material.

Due to the questionable validity of applying analytical results to surrounding material, it was necessary either to further increase the number of samples per plate or to develop a nondestructive analytical technique applicable to the core blank itself.

FIGURE 25. Sampling Plan and Analyses on Rolled Plates A19 and A20

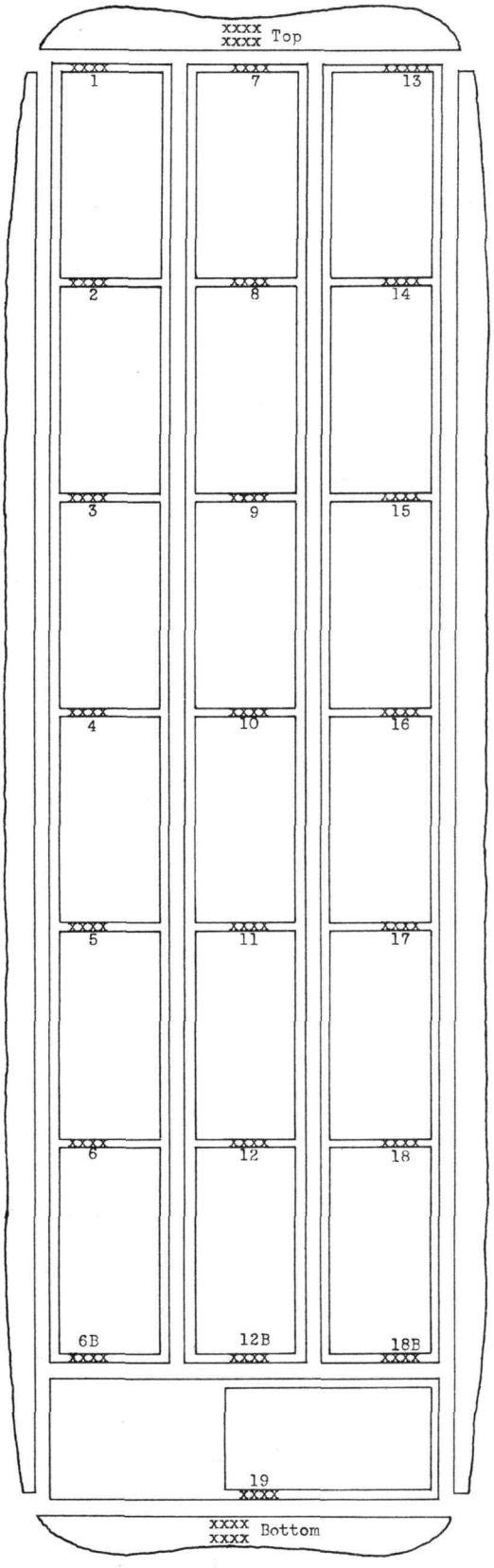

Sample No.	w/o Uranium	
	Plate No. 19	Plate No. 20
1	18.99	19.09
2	17.51	17.98
3	17.44	17.64
4	17.39	17.66
5	17.56	17.72
6	17.29	17.72
6B	17.58	17.84
7	19.81	24.89
8	17.64	17.68
9	17.97	19.06
10	18.22	18.58
11	17.70	17.84
12	17.62	17.78
12B	19.49	17.90
13	19.06	23.63
14	17.54	17.25
15	17.32	17.51
16	17.83	17.60
17	17.47	17.76
18	17.38	17.66
18B	17.46	17.86
19	17.76	18.10

	Plate No. 19		Plate No. 20	
	Top	Bottom	Top	Bottom
w/o Iron	0.34	0.42	0.41	0.43
w/o Nickel	1.53	1.98	1.75	1.85

An attempt at using X-ray emission spectroscopy methods for determining uranium content was made, as this method gave results much more rapidly than by wet chemistry analysis. Thus an increased number of samples would be offset by the savings in analytical time. Again, however, the problem of segregation in a solid sample was present. Emission spectroscopic work showed definite segregation in the sample itself. While this analytical method is applicable to solution as well as to solid samples, it was felt that dissolution of the solid samples to eliminate segregation would destroy the time-saving benefit of this method in addition to lowering the accuracy of the results. As this method still involved the problem of applying analytical results of surrounding material to the core blank proper, emission spectroscopic analysis was rejected in favor of a nondestructive method.

In conjunction with the analytical work, density and hardness measurements were made to determine if there was sufficient correlation with uranium content to determine the uranium content of a core blank.

Density determinations were made by measuring the volume of the sample by means of immersion in carbon tetrachloride. The difference between mass determined in air and mass measured by immersion in CCl_4, the density of CCl_4 as a function of temperature, and the sample mass in air gives sufficient data to calculate the sample density.

Hardness was measured on a Rockwell Superficial Tester with the 15-T scale employing a $\frac{1}{16}$-in. diameter hardened steel ball and a 15-kg major load.

The samples used for hardness and density measurements were taken from plates A19 and A20, using the lattice strips between the punched core blanks. After making hardness and density measurements, the pieces were cut up and used as analytical samples for uranium analysis.

Table VI lists the hardness and density data for the samples, together with the uranium content. The hardness values show no apparent correlation with uranium content. There is some doubt as to the accuracy of the hardness data, since there was difficulty in obtaining reproducible values in some pieces.

Although the density data show some correlation with uranium content, this was not sufficient to justify its use as a measure of uranium content of a core blank. As the alloy consists of more than one phase, each of differing density, the overall density of the material is affected by the amount of various phases present. As will be shown later, metallographic studies revealed a vast difference in structure between the top and bottom of a casting, due to the difference in cooling rate. While this variance in cast structure was greatly reduced through fabrication, there still existed a difference in

TABLE VI. Density and Hardness Values for Samples with Known Uranium Content

Plate A19				Plate A20			
Analytical Sample No.	U, w/o	Density, gm/cc	Hardness* Rockwell, 15-T	Analytical Sample No.	U, w/o	Density, gm/cc	Hardness* Rockwell, 15-T
1	18.99	3.205	48.2	1	19.09	3.188	34.2
2	17.51	3.166	62.4	2	17.98	3.171	45.5
3	17.44	3.178	60.0	3	17.64	3.144	-
4	17.39	3.192	60.0	4	17.66	3.166	50.3
5	17.56	3.185	60.9	5	17.72	3.172	55.8
6	17.29	3.180	62.7	6	17.72	3.174	52.2
6B	17.58	3.196	-	6B	17.84	3.196	60.7
7	19.81	3.226	-	7	24.89	3.358	49.1
8	17.64	3.164	-	8	17.68	3.163	46.6
9	17.97	3.188	-	9	19.06	3.198	44.6
10	18.22	3.197	-	10	18.58	3.198	46.4
11	17.70	3.185	-	11	17.84	3.170	47.4
12	17.62	3.176	-	12	17.78	3.165	50.1
12B	19.49	3.191	-	12B	17.90	3.194	59.5
13	19.06	3.206	-	13	23.63	3.325	51.0
14	17.54	3.170	-	14	17.25	3.146	43.9
15	17.32	3.174	-	15	17.51	3.158	47.6
16	17.83	3.190	-	16	17.60	3.165	49.2
17	17.47	3.177	-	17	17.76	3.152	-
18	17.38	3.178	-	18	17.66	3.171	53.2
18B	17.48	3.195	-	18B	17.86	3.201	60.2
19	17.76	3.207	-	19	18.10	3.204	61.7

*Average of three readings.

structure which could affect density. Of equal importance is the possibility of microporosity, which is prevalent in aluminum and aluminum alloys and which could cause a variation in observed density.

Since a nondestructive determination of uranium content on a core blank itself was most desirable, work was done to evaluate the method of determining U^{235} content of a core blank by counting the number of gamma-ray emissions per unit of time. Although the number of emissions is not a linear function of uranium content, linearity may be assumed over the small range of uranium content in question.

The relationship between the number of counts and U^{235} content was established by counting three core blanks of different analyses. One core blank approximated the desired 39 gm U^{235} while the other two were selected as representing approximately 37.5 and 41 gm, slightly outside the specified content of 39 ± 1 gm. These core blanks were counted a number of times to establish an accurate count of emissions in a five-minute

counting period and to insure reproducibility. The counting method, in effect, resolved the counts of the material to give an average count for the core blank as a whole and eliminated the problem of minor segregation. The three core blanks were completely dissolved and analyzed to give an average uranium content for the total core blank. The number of counts recorded per unit time and the average U^{235} content of these core blanks provided a standard by which a core blank of unknown U^{235} content could be nondestructively analyzed by counting the number of gamma emissions in the given counting period. Any major segregation in a core blank which might affect the reliability of this method would be easily detected through X-ray radiography.

A detailed discussion of the theory pertaining to this method and the experimental determination of its feasibility are reported in ANL-5944.(4)

X-ray Radiography

X-ray radiographs of punched core blanks showed definite areas of segregation in the top section of each plate. There also existed a variance in microstructure, which also was reflected in the uniformity of the radiographs.

Radiographs of a casting showed a segregated area at the junction between the hot top and the body of the casting, this area and the hot top being the last to solidify. With the hot top zone remaining molten, maximum formation of hypereutectic UAl_3 (with a peritectic transformation to UAl_4) occurred, thereby depleting the remaining liquid alloy of uranium. Final solidification occurred at the top when the eutectic composition (13 w/o U) and temperature (640°C) were reached. A high uranium concentration would be expected at the area rich in primary UAl_3 crystals, and a low U content in the region of eutectic solidification. An analysis of casting A9 showed the uranium content to be 18.32 w/o at the juncture between the casting and hot top, and 10.71 w/o in the upper portion of the hot top.

This area of high uranium segregation extended deeply enough into the body of the casting so as to be present after removal of the hot top, and consequently appeared in the top of the rolled plate. This area normally existed in the top row of punched core blanks, and the two side core blanks in particular. All core blanks rejected in X-ray radiography were from the top area of the plate, where this segregation occurred.

X-ray radiographs of core blanks punched from the bottom area of the plate showed a more uniform appearance than did the top core blanks, which tended to appear mottled in structure. This resulted from the temperature gradient in the mold and the rate of solidification of the casting. The bottom of the casting, solidifying and cooling much more rapidly than the top, showed a finer phase dispersion and grain size than did the top. The finer structure appeared more uniform in a radiograph.

Ultrasonic Transmission Testing

The initial nondestructive testing program for core blanks did not include an ultrasonic test for core blank soundness and homogeneity, as it was felt that X-ray radiography furnished sufficient data. With the advent of fuel plate fabrication and the initial high reject rate encountered in ultrasonic testing of fuel plates, a series of reject plates were sectioned through the reject area and microscopically examined. The cause for rejection, initially thought to be an unbonded area between core and cladding, resulted from major cracks appearing in the core in the plane of the fuel plate. These cracks were readily visible to the naked eye. The punched core blanks used in fabrication of these defective plates all were acceptable on the basis of X-ray radiography prior to assembly into fuel plate composites.

It was then decided that all core blanks would be given an ultrasonic transmission test to reject core blanks with internal cracks or areas likely to crack in fuel plate fabrication. Initial testing was run at as high a sensitivity as possible while allowing the beam to pass through the core blank. Three rejected core blanks were sectioned through their defects and examined microscopically. No definite evidence could be found to cause rejection, although there did seem to be slight evidence indicating a banded structure in the direction of rolling. This appearance was not pronounced nor definitely established.

Later work indicated that a lower level of sensitivity could be used and still obtain rejection of core blanks possessing cracks or major defective areas. The less sensitive test did reduce the number of reject core blanks. Most of the sonic reject core blanks were associated with the top row of core blanks, the same core blanks rejected for segregation or a U^{235} content beyond specifications.

Metallography and X-ray Diffraction

In conjunction with the nondestructive testing of the core blanks, a casting containing normal uranium was cast and fabricated in the same manner as the enriched castings to provide material for metallographic and X-ray diffraction studies.

Two $\frac{1}{8}$-in. thick slices were cut from the conditioned casting, one slice taken from the top and the second from the bottom. Metallographic samples from the two edges and center of each slice were examined, and the remaining material was used for X-ray diffraction studies. The casting was then rolled according to the schedule for enriched material, and samples were again taken from the top and bottom for metallography and X-ray diffraction.

The metallographic samples were polished mechanically and etched with a 0.5% HF solution. Photomicrographs of the as-cast material are shown in Figure 26.

The effect of the mold temperature gradient on the as-cast structure is readily apparent. The bottom edges of the casting show a fine dispersion of UAl_4 particles in an eutectic and aluminum matrix. The bottom center of the casting, having cooled more slowly than the edges, shows a greater amount of UAl_4 particles in the matrix; the particles are much larger and have lost much of the geometric appearance characteristic of the particles at the edges. At the top of the casting, where the solidification rate was slowest, the UAl_4 particles are massive and the patches of eutectic are very coarse in appearance. There is no change in microstructure from the edges to center at the top as the mold was sufficiently hot to prevent the formation of a "chilled" zone characteristic of the edges at the bottom.

The microstructure of the rolled plate, shown in Figure 27, is essentially similar, except that the UAl_4 particles have become fragmented during rolling and have lost their crystalline appearance. There also appears to be a dispersion of fine particles throughout the matrix, these particles possibly being an uranium carbide or nitride or a nickel-aluminum compound ($NiAl_3$) formed during the hot working of the casting. The temperature and deformation encountered in the hot rolling of the billet would promote diffusion and subsequent precipitation.

While much of the difference in structure between the top and bottom of the casting has been eliminated by the fabrication procedure, the rolled plate still exhibits a larger UAl_4 particle size and less uniform dispersion at the top than at the bottom.

X-ray patterns were taken on solid material by the diffractometer chart method, and by the powder camera method on scrapings from the rolled plate. The powder camera method was used on rolled material only while the diffractometer method was run on both as-cast and rolled samples.

A tabulation of the X-ray diffraction results is shown in Table VII. All samples showed a UAl_4 phase in an aluminum matrix. Weaker phases such as UO_2, UAl_3, U (N or C), and $NiAl_3$ were possibly present, but the weakness of the line intensities makes their identification questionable.

While the as-cast sample from the top showed no UAl_3 phase, there is a possibility of its existence in the bottom sample of as-cast material. As the peritectic composition of the U-Al system lies between 15 and 17 w/o U, solidification of a 17.5 w/o uranium-aluminum alloy would begin with the formation of UAl_3, with a later transformation to UAl_4. The rapid rate of solidification occurring at the bottom of the mold would tend to inhibit the transformation of UAl_3 to UAl_4, while the slow solidification rate at the top would allow complete transformation. The possible presence of UAl_3 in the

FIGURE 26. Photomicrographs of Samples from Top and Bottom of a Typical Casting. Etched in 0.5% HF Solution; 250X Magnification

A

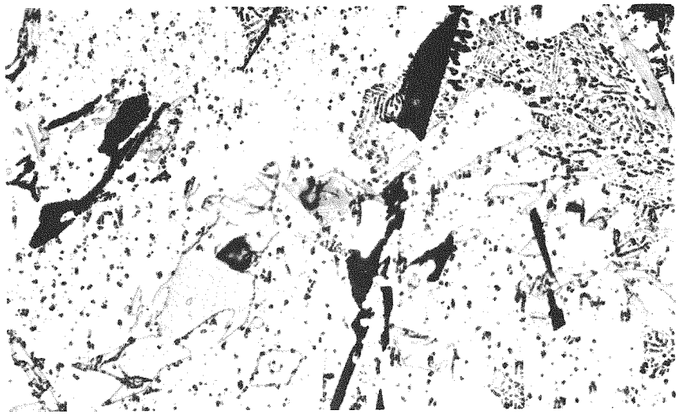

B

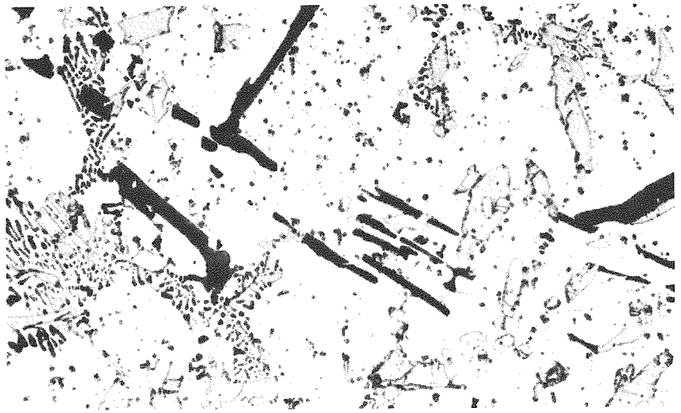

C

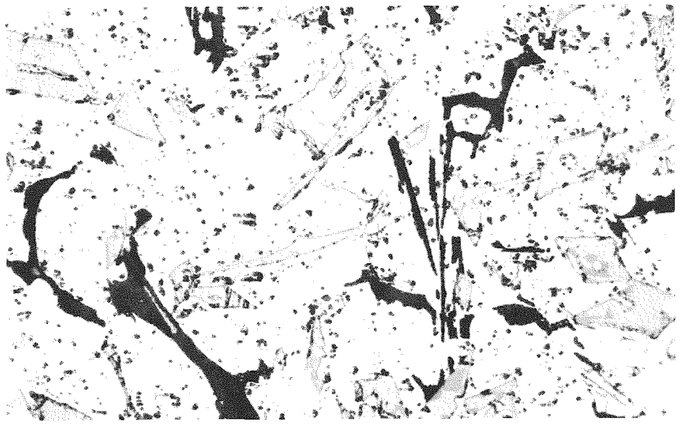

24076

Top Samples

A

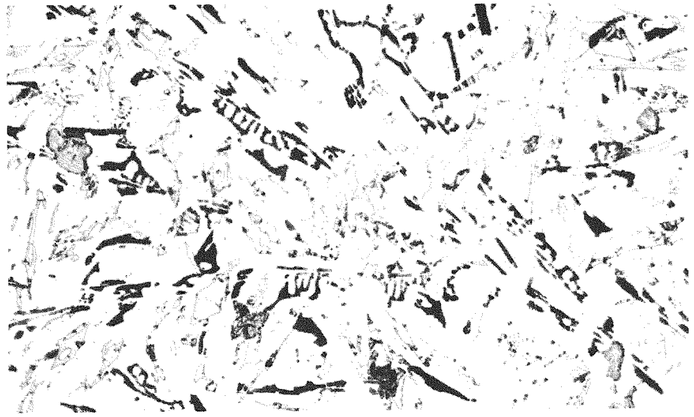

B

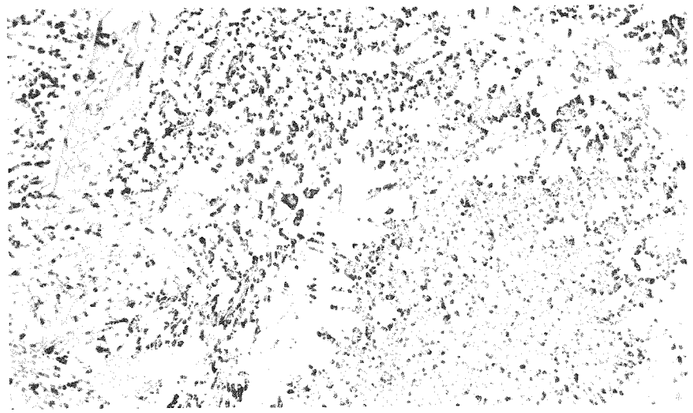

C

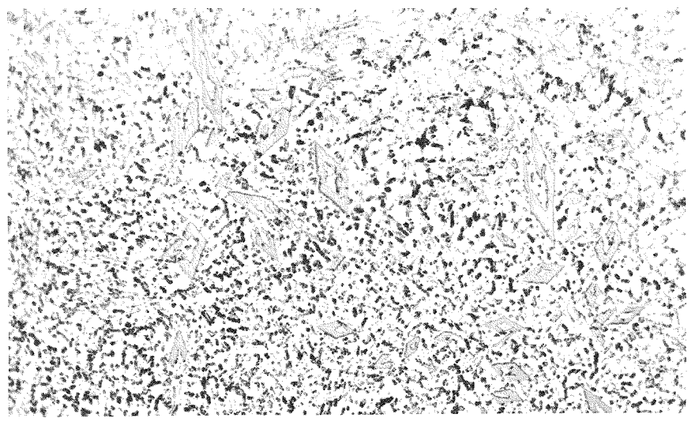

24080

Bottom Samples

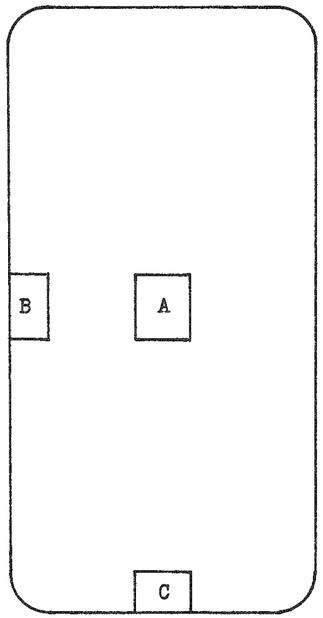

Location of sample in cross-sectional slice.

FIGURE 27. Photomicrographs of Samples from Top and Bottom of a Rolled Plate. Etched in 0.5% HF solution.

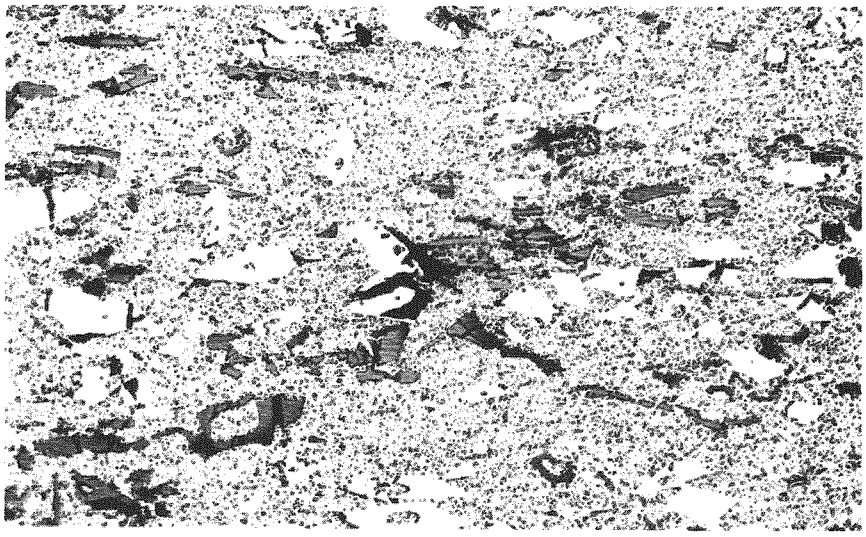

24378 Top 250X

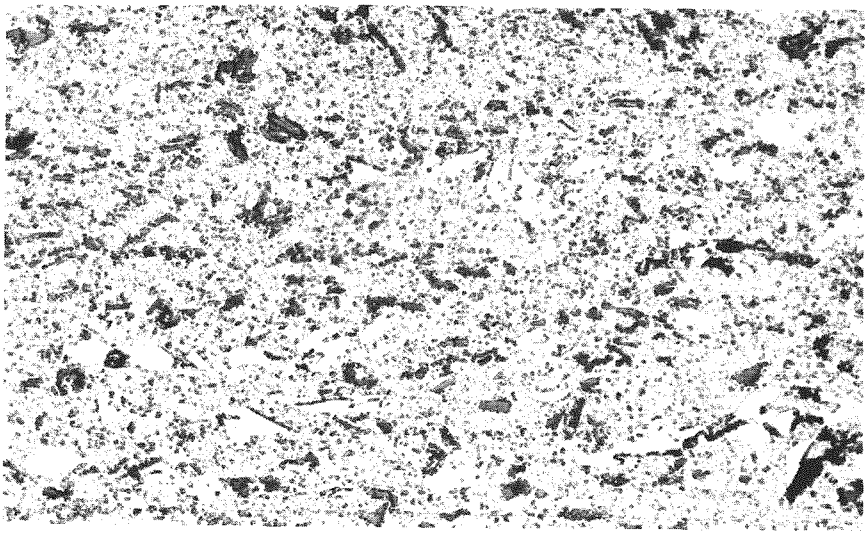

24379 Bottom 250X

TABLE VII. X-ray Diffraction Patterns of ALPR Material

Sample	Type of Pattern	Phases*
Cast - top	Diffractometer Chart	s-Al, m-UAl_4, vw-UO_2
Cast - bottom center	Chart	s-Al, m-UAl_4, w-UAl_3, w-UO_2, vw-U(N or C), vw-$NiAl_3$?
Cast - bottom edge	Chart	s-Al, s-UAl_4, w-UAl_3, w-UO_2, vw-$NiAl_3$?
Rolled - top	Chart	s-Al, m-UAl_4, w-UAl_3, w-UO_2, vw-U(N or C), vw-$NiAl_3$?
Rolled - top	Film	s-Al, m-UAl_4, w-UO_2, vw-U(N or C)
Rolled - bottom	Chart	s-Al, s-UAl_4, m-UO_2, w-U(N or C), vw-UAl_3, w-$NiAl_3$?
Rolled - bottom	Film	s-Al, m-UAl_4, w-UO_2, vw-U(N or C)

*s - strong; m - moderate; w - weak; vw - very weak

top of the rolled plate, as indicated by the diffractometer chart, is not explainable, nor is the presence of $NiAl_3$ in cast material from the bottom. The results from the powder camera method showed only a weak presence of these phases, and it is possible that the small amount of scrapings necessary for the powder method may not have included these phases.

EVALUATION OF MANUFACTURING PROCESSES

As this aluminum-uranium alloy or similar alloys have been used for a number of reactor loadings, a discussion of process yields is included for evaluation of the operations and to determine where yields can be improved. A tabulation of process yields at the major stages of manufacture is given in Table VIII.

TABLE VIII. Tabulation of Process Yields at Various Stages of Manufacture

Stage of Manufacture	Total Weight of Material (gm)	Percent of Total Charge Weight
Charge Materials	559,375.34	100.0
Castings	550,265.73	98.4
Conditioned Billets	429,674.37	76.1
Punched Core Blanks (1150)	276,549.25	49.4
Acceptable Core Blanks (851)	203,681.80	36.4

Uranium Preparation

As it was found necessary to process the as-received biscuit uranium to remove impurities causing porosity in castings, the uranium was melted in vacuum and cast into bars which were cut into segments for charging to the alloy melts. An overall flow sheet for the preparation of uranium is shown in Figure 28.

Of the initial 56.72 kg of biscuit uranium, 3.93 kg were charged to ALPR melts in the as-received condition. In an attempt to eliminate porosity in ALPR castings, the biscuit uranium was pickled to remove the heavy oxide and surface impurities. A total of 7.19 kg was pickled; 4.36 kg being charged to ALPR melts, 2.81 kg later remelted, and the remaining 0.02 kg being in the nitric acid pickle solution. A total of 48.92 kg of uranium was premelted, including 5 gm of foil to prevent magnesium deposition on the mold walls and 497 gm of cast uranium remelted. Of the total charge material, 97½% was recovered as usable cast material and the remaining 2½% was scrap in the form of shot and skull. From 47.7 kg of cast material, 43.27 kg (90.17%) were charged to ALPR, 0.50 kg were remelted, and 3.93 kg remained as scrap from machining and breaking. Out of the original 56.72 kg of biscuit uranium received and an additional 2.00 kg of premelted material, 53.56 kg, or 91.21% was charged to the ALPR melts.

ALPR Charging and Casting

Figure 29 is a flow sheet of a material balance on the casting and fabricating of ALPR core blanks for fuel plate production. In 68 heats, a total of 559.38 kg were charged, of which 54.75% was virgin material and 45.25% was remelt stock. The high percentage of remelting resulted because nine castings were remelted due to porosity and a low yield of acceptable fuel plates. A total of 1150 core blanks were punched to give 816 acceptable core blanks necessary to fabricate 594 required fuel plates.

Of the total charge weight, 98.37% (550.26 kg) was recovered in castings.

FIGURE 28. Preparation and Material Balance of Uranium Charged to ALPR Melts

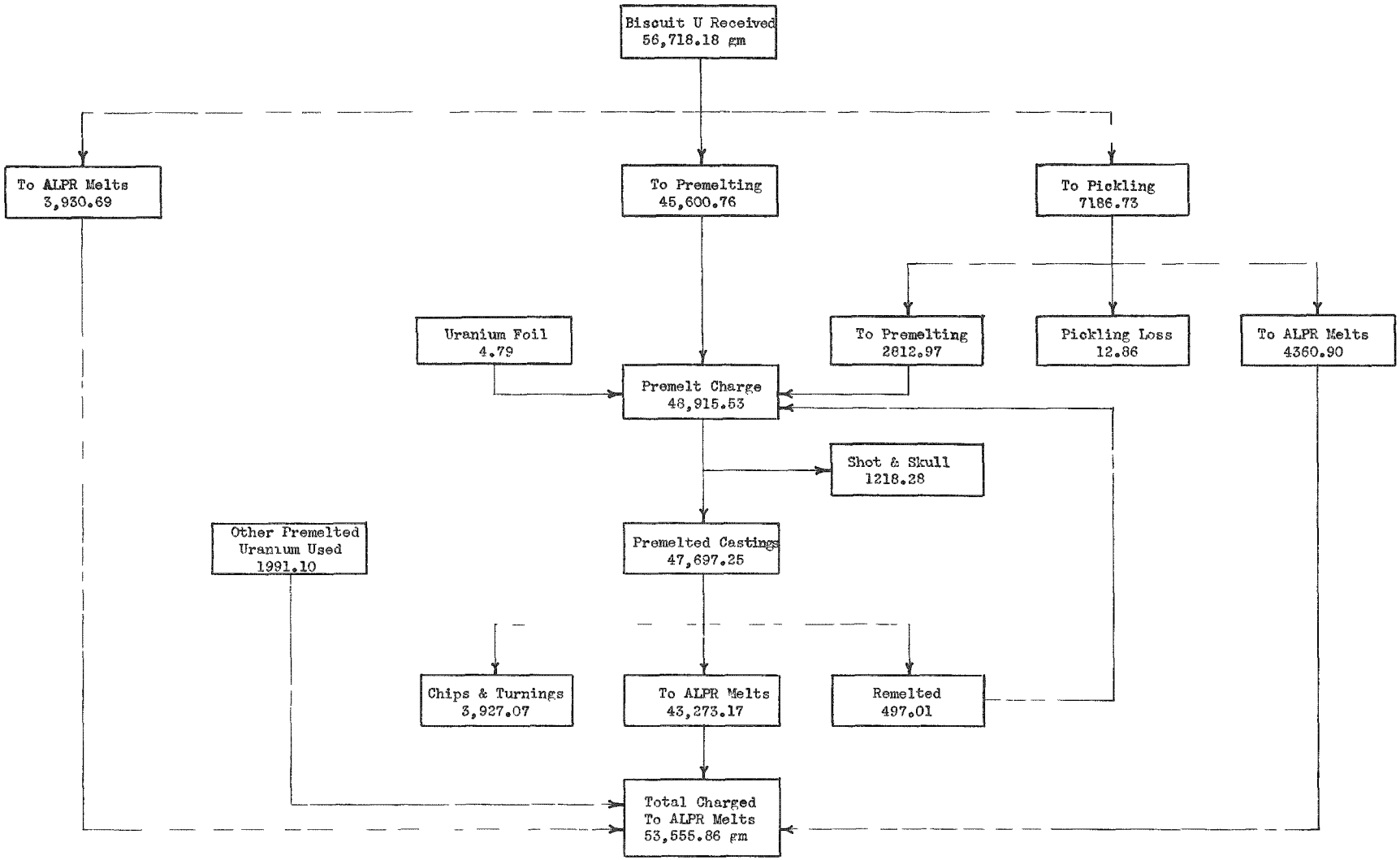

FIGURE 29. Material Balance on Casting and Fabricating Core Blanks for ALPR Fuel Plate Production

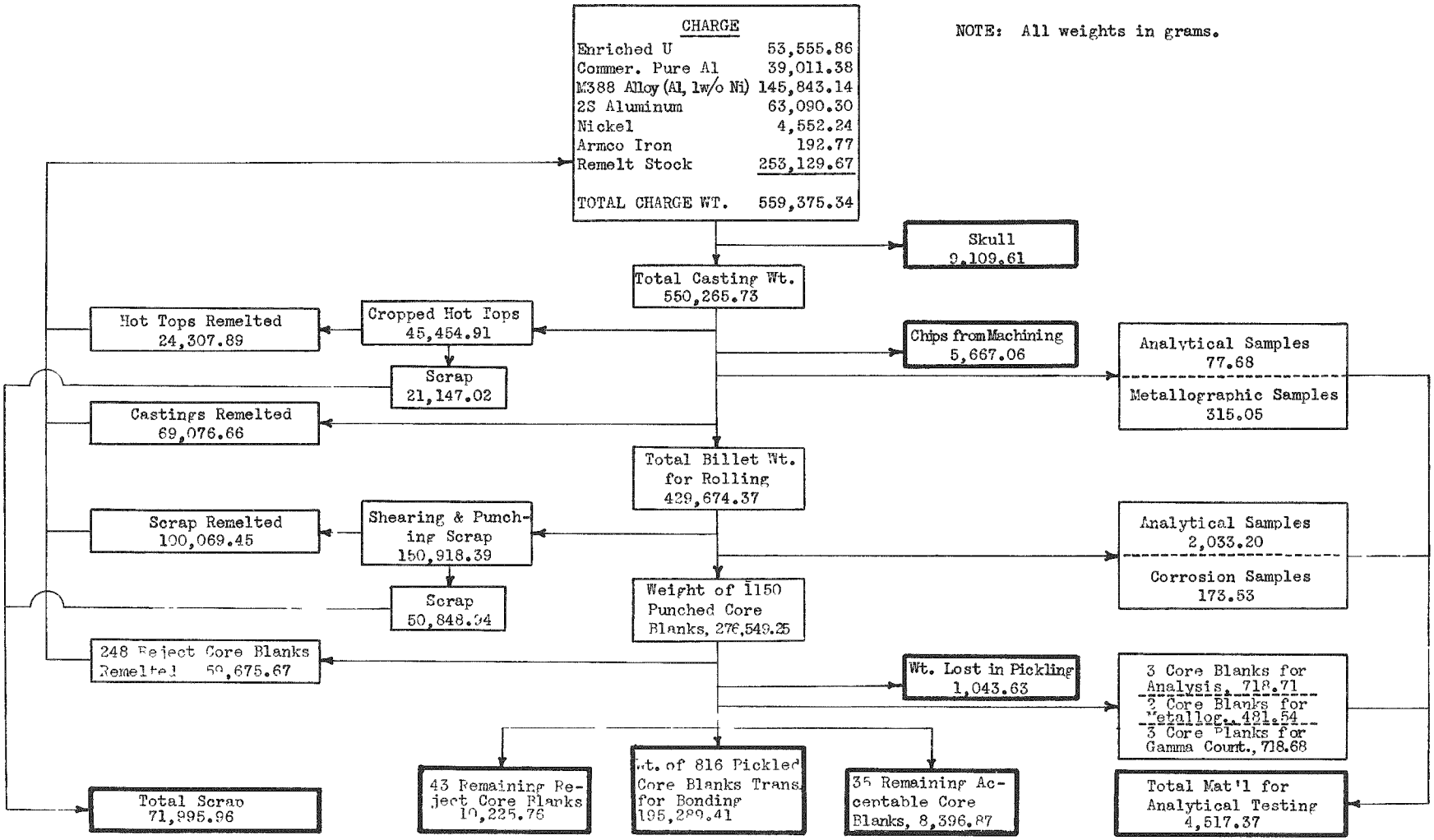

Billet Conditioning

A total of 68 castings were conditioned, from which 59 billets weighing 429.67 kg were fabricated to realize a yield of 78.08% of the total cast weight. Nine castings weighing 69.08 kg (12.55% of total casting weight) were remelted due to porosity. Hot tops cropped from the casting weighed 45.45 kg and constituted 8.26% of the casting weight. Of this weight, 24.31 kg were remelted and the remaining 21.14 kg of hot tops were classified as scrap at the end of the project, although they were suitable for remelting. Of the remaining material, 0.39 kg (0.08%) was used for analytical and metallographic samples and 5.67 kg (1.03%) remained as scrap chips from machining.

The major factor in the low yield of billet weight to total casting weight was the nine castings which were remelted Eight castings were made with biscuit uranium that was not premelted. Considering only the 60 billets cast from charge material utilizing premelted uranium, a billet yield of 88.31% was realized; a significant increase over the actual yield of 78.08%

Similarly, the total scrap at the end of the project would have been reduced considerably had the remaining hot tops been used as remelt stock.

Core Blank Punching

A total of 1150 core blanks weighing 276.55 kg were punched from the 59 rolled plates to give a 64.36% yield. Analytical samples represented 0.52% of the total weight and, of the remaining 35.12%, 23.29% represented 100.07 kg of sheared scrap that was remelted and 11.83%, the 50.85 kg of sheared material, classified as scrap. The latter material was acceptable for remelting but was retained in the event that future analytical work might require this trellis work surrounding the punched core blanks.

While this yield of 64 36% is low, no significant improvement can be made due to the configuration at the ends of the rolled plate and the necessity of material surrounding each core in the punching operation. A slight increase would have been possible had the initial casting been $\frac{1}{2}$ to 1 in. longer. This increase in length would have increased the rolled plate length such that 21, rather than 19, core blanks could be punched. Plates from which 21 core blanks were punched realized yields of approximately 69.5% as opposed to 64.0% for plates from which only 19 core blanks were punched.

Core Blank Evaluation and Disposition

A breakdown of core blank testing and disposition is shown in Table IX. Of the total 276.55 kg of 1150 punched core blanks, 71.0% (816 core blanks) were fabricated into fuel plates. Two hundred and forty-eight core blanks

TABLE IX. Evaluation of Core Testing and Disposition of Core Blanks

Casting No.	Cores Punched	X-ray Evaluation		Ultrasonic Testing		U^{235} Content by γ Emission		Core Blank Disposition				
											Remaining	
		No. X-rayed	Acceptable	No. Tested	Acceptable	No. Counted	Acceptable	Fuel Plate Fabrication	Remelted (Rejects)	Analytical Work	Acceptable	Rejected
A-9	10	10	8	-	-	8	8	8	2	-	-	-
A-10	19	19	16	2	2	12	11	16	3	-	-	-
A-11	19	19	19	2	2	19	18	16	2	1	-	-
A-12	19	19	17	-	-	19	19	14	4	1	-	-
A-13	19	19	15	1	0	19	13	13	5	1	-	-
A-14	19	19	19	-	-	19	19	18	1	-	-	-
A-15	19	19	18	2	0	19	17	16	3	-	-	-
A-16	19	19	18	-	-	19	19	18	1	-	-	-
A-17	19	19	18	-	-	19	16	15	4	-	-	-
A-18	19	19	17	3	3	19	19	17	2	-	-	-
A-19	19	19	16	-	-	19	19	13	6	-	-	-
A-20	19	19	14	-	-	19	17	14	5	-	-	-
A-21	19	19	17	1	1	19	15	14	5	-	-	-
A-22	19	19	16	-	-	19	15	13	5	1	-	-
A-23	18	18	16	3	2	18	15	13	5	-	-	-
A-24	19	19	16	1	1	19	17	16	3	-	-	-
A-25	19	19	18	1	0	19	16	13	6	-	-	-
A-26	19	19	16	2	0	19	15	13	6	-	-	-
A-27	19	19	17	1	0	19	15	13	6	-	-	-
A-28	19	19	17	1	0	19	18	15	4	-	-	-
A-29	19	19	16	10	5	19	18	9	10	-	-	-
A-30	19	19	16	15	14	19	15	14	5	-	-	-
A-31	19	19	16	16	11	19	18	9	10	-	-	-
A-32	19	19	16	14	9	19	18	19	9	-	-	-
A-33	19	19	17	16	13	19	18	13	5	-	-	1
A-34	19	19	16	16	12	19	16	11	8	-	-	-
A-35	19	19	17	16	13	19	19	13	6	-	-	-
A-36	19	19	18	17	14	19	17	13	6	-	-	-
A-37	19	19	18	2	1	19	15	12	6	1	-	-
A-38	19	19	16	1	1	19	18	15	4	-	-	-
A-39	19	19	16	4	4	19	17	16	3	-	-	-
A-40	19	19	17	17	12	19	18	12	6	1	-	-
A-41	19	19	16	14	12	19	18	15	4	-	-	-
A-42	19	19	19	18	15	19	18	16	3	-	-	-
A-43	-*	-*	-	-	-	-	-	-	-	-	-	-
A-44	21	21	18	-	-	21	18	0**	21	-	-	-
A-45	21	21	19	15	11	21	17	12	9	-	-	-
A-46	18	18	18	18	14	18	18	14	3	-	-	1
A-47	20	20	17	18	18	20	18	17	1	1	-	1
A-48	19	19	17	17	17	19	19	16	2	-	1	-
A-49	21	21	18	18	18	21	21	18	3	-	-	-
A-50	21	21	19	19	14	21	19	11	9	-	1	-
A-51	20	20	16	20	17	20	14	9	11	-	-	-
A-52	21	21	20	21	21	21	20	18	2	-	1	-
A-53	21	21	18	21	20	21	21	18	3	-	-	-
A-54	21	21	19	21	18	21	19	14	7	-	-	-
A-55	21	21	18	21	21	21	21	18	3	-	-	-
A-56	21	21	19	21	20	21	21	18	3	-	-	-
A-57	21	21	18	21	19	21	21	16	4	-	-	1
A-58	21	21	19	21	21	21	17	15	4	-	-	2
A-59	21	21	17	21	20	21	18	12	-	-	2	7
A-60	21	21	19	21	21	21	20	18	-	-	1	2
A-61	17	17	15	17	17	17	15	13	-	-	-	4
A-62	21	21	18	21	19	21	21	14	-	-	2	5
A-63	21	21	18	21	18	20	18	14	-	1	1	5
A-64	21	21	19	21	21	21	19	19	-	-	-	2
A-65	21	21	19	21	19	21	19	17	-	-	-	4
A-66	21	21	19	21	21	21	21	11	-	-	8	2
A-67	21	21	20	21	21	21	18	10	-	-	8	3
A-68	21	21	19	21	21	21	18	8	-	-	10	3
TOTAL	1150	1150	1018	674	594	1140	1035	816	248	8	35	43

*Casting was porous and remelted.
**Core blanks remelted due to low content of Fe.

(21.6%) were rejected by one or more of the nondestructive tests and were remelted. Analytical work accounted for eight core blanks (0.7%). There remained a total of 78 core blanks (6.7%) of which 43 were rejects and considered scrap, while the remaining 35 were acceptable for use in fuel plate fabrication. Of the 1150 core blanks punched, 851 (74.0%) were acceptable.

All the punched core blanks were X-ray radiographed and 1018 (88.6%) were acceptable. Out of 674 tested by ultrasonics, 594 (88.2%) were acceptable. Similarly, a total of 1140 core blanks were analyzed for U^{235} content by gamma-emission counting and 1035 (90.8%) were within the specified limits.

As all punched core blanks did not undergo all three nondestructive tests, a definite correlation between the tests would be incomplete. A general pattern was evident, however, and indicated that core blanks rejected for segregation by X-ray radiography would also be rejected in ultrasonic testing and by gamma-emission counting for a U^{235} content beyond specifications. While other core blanks would occasionally be rejected by one or more of the tests, the bulk of the rejected core blanks were those from the top row where segregation existed.

SUMMARY

Figure 30 is an overall flow sheet schedule for production of fuel core blanks. While 36.4% recovery of acceptable core blanks from the total weight charged to the melting furnace is extremely low, this figure reflects the amount of material recycled during production. The 203.68 kg of fuel material (851 acceptable core blanks) constitutes 66.5% actual yield from 306.25 kg of virgin material charged to the 68 heats. Over 45% of the total charge weight consisted of remelt stock generated in processing.

On the basis of material charged to ALPR fuel core manufacture, 66.5% was recovered as acceptable core material 1.5% was used in analytical work, and 5.2% was classified as unusable scrap. The remaining 26.8% is material suitable for recovery by remelting.

There are three main areas in which better utilization of material and processes could be employed.

(1) Proper design of a mold such that a segregated zone will not occur in the material intended for rolling. Had this zone been completely eliminated from the conditioned billet, the yield of acceptable core blanks would have been materially increased as segregation normally rejected the top row of core blanks.

FIGURE 30. Flow Sheet for ALPR Fuel Plate Core Blank Production

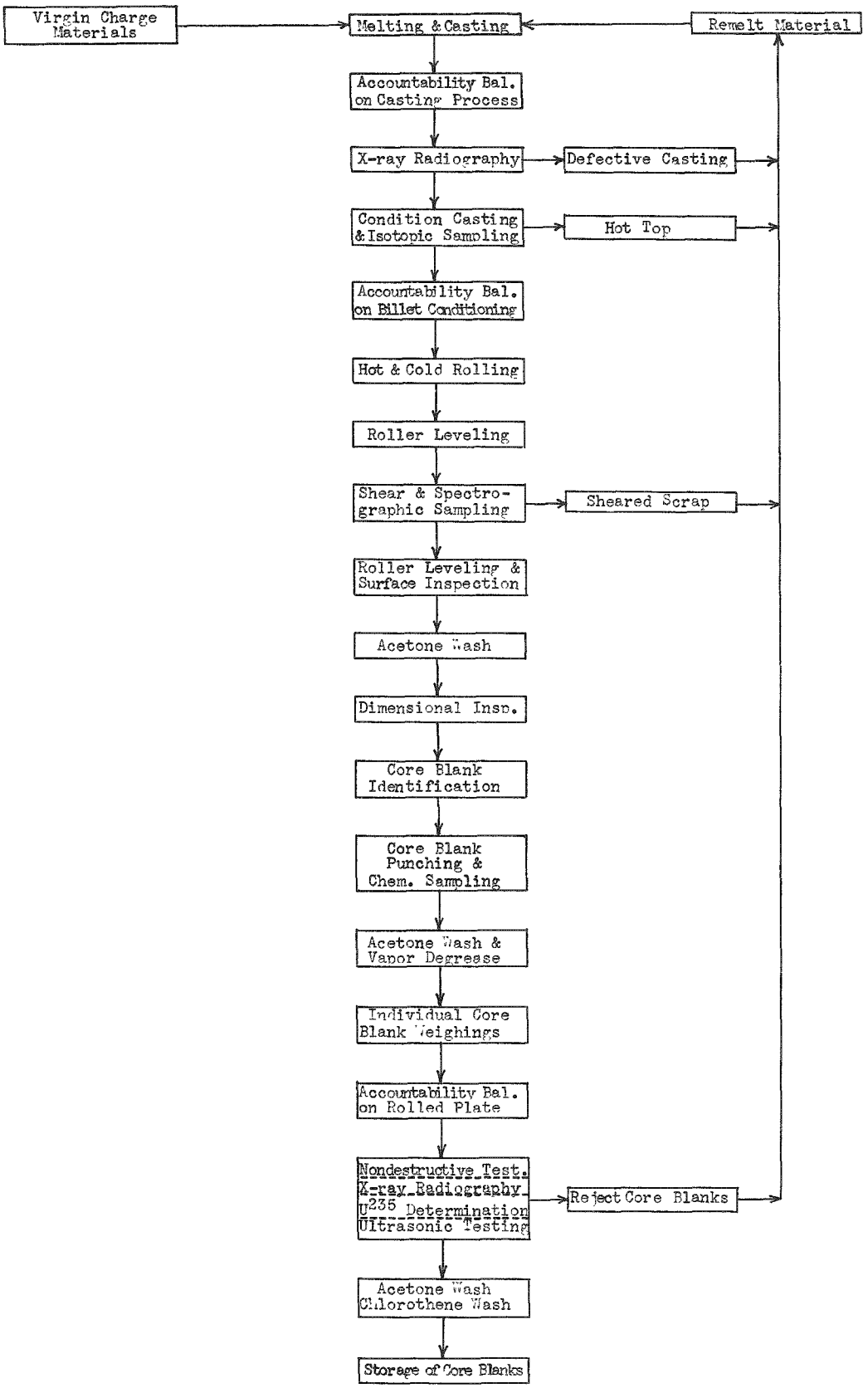

(2) Better scheduling of manufacture would have enabled a greater portion of material to be used. As mentioned earlier, 26.8% of the raw material charged remained as processing scrap suitable for remelting.

(3) Recovery of core material from the rolled plate could be increased. Due to the configuration of the rolled plate and the necessity for a frame from which to punch core blanks, only 64.4% of the rolled plate weight was recovered as punched core blanks.

The use of a process such as extrusion in which core material could be directly sized in two dimensions from an extrusion billet, would greatly reduce the amount of scrap generated in core blank fabrication.

ACKNOWLEDGEMENTS

The fabrication of core material for ALPR fuel plate fabrication involved the efforts of many individuals to whom the authors are indebted.

Thanks go to R. E. Macherey, for his able guidance of the project and review of the manuscript.

Spectrochemical and uranium analyses were performed by J. A. Goleb and H. B. Evans of the Chemistry Division and the personnel under them.

The inspection of core blanks was based on radiography, ultrasonic and gamma emission testing ably done by the Nondestructive Testing Group under W. J. McGonnagle.

Machining of premelted uranium and conditioning of ALPR castings were done by R. J. Pershey and L. L. Peterson from Central Shops.

Production of uranium castings and ALPR castings was done by J. A. Zic, L. Hanna, C. A. Bogenschneider, D. L. Hoffman, and R. R. Langel. Under the direction of R. A. Beatty, the rolling of billet material was performed by F. J. Karasek, C. Steves, A. C. Carr, D. L. Hoffman, and H. C. Glienke. The fine performance by these technicians of the Foundry and Fabrication Group of the Metallurgy Division is gratefully acknowledged.

The photographs in this report were taken by C. L. Long of Graphic Arts.

Special thanks are due to Regina A. Wanda for compilation of data and preparation of the manuscript.

REFERENCES

(1) R. A. Noland, D. E. Walker, and M. M. Martin, The Manufacture of Fuel Plates and Fuel Subassemblies for the Argonne Low Power Reactor (ALPR), ANL-5965 (to be published).

(2) W. B. Haynes and F. R. Lorenz, Preparation of Uranium Alloys by Melting, WAPD-PWR-FEM-106 (February 1956).

(3) R. E. Macherey et al., Manufacture of Fuel Plates for the Experimental Boiling Water Reactor, ANL-5629 (June 1957).

(4) W. J. McGonnagle and R. B. Perry, Analysis of Fuel Element Core Blanks for Argonne Low Power Reactor by Gamma Counting, ANL-5944 (to be published).

(5) W. J. McGonnagle, W. N. Beck and N. P. Lapinski, Inspection of Fuel Element Components and Fuel Elements for the ALPR, ANL-5951 (August 1959).